1979

The effects of air content, water-cement ratio, and aggregate type on the flexural fatigue strength of plain concrete

Thomas Lee Thomas
Iowa State University

The effects of air content, water-cement ratio, and aggregate type on the flexural fatigue strength of plain concrete

by

Thomas Lee Thomas

A Thesis Submitted to the

Graduate Faculty in Partial Fulfillment of

The Requirements for the Degree of

MASTER OF SCIENCE

Department: Civil Engineering
Major: Structural Engineering

Approved:

Signatures redacted for privacy.

Iowa State University
Ames, Iowa

1979

TABLE OF CONTENTS

LIST OF TABLES

LIST OF FIGURES

INTRODUCTION

Fatigue of Concrete

If repetitive loads cause stresses and strains above a certain critical value (fatigue limit), structural damage may develop and progress until failure occurs; failure can occur at stresses considerably less than the static ultimate strength. When a material fails under a number of repeated loads, each smaller than the static ultimate strength, failure is classified as a fatigue failure. Fatigue damage depends upon the applied stress level and the number of load applications. It is therefore important to quote fatigue strength for a specified number of cycles of loading when discussing the fatigue properties of a material. Fatigue strength is defined as the stress causing failure after a stated number of cycles of loading. Fatigue life is the number of cycles of a specified stress that a specimen can withstand without failure.

Fatigue research followed field problems after fatigue was suspected as a cause of failure. One of the earliest studies was conducted in 1829, when mine-hoist chains were subjected to repeated proof loadings. Railway companies were interested in practical problems such as bridge construction and the fatigue of railway vehicle axles, however interest in fatigue of nonmetals lagged for 40 years.

The first study involving concrete flexural specimens was conducted by Féret in 1906 (27). This investigation was part of a broader study including plain and reinforced mortar beams, cubes, and cylinders and thus is of historical interest only.

Tests by Van Ornum, using concrete beams reinforced with 2-1/2% steel, determined the flexural fatigue limit to be 50 percent of the modulus of rupture under progressive loading (24). All of Van Ornum's tests showed that as the fatigue load was increased above 50 or 55 percent of the modulus of rupture, the number of repetitions of load to cause failure was rapidly reduced.

The first investigations on flexural fatigue of concrete of significant consequence were carried out almost simultaneously by the Illinois Department of Highways (1921-23) and Purdue University (1922-24). The Illinois highway officials observed that failures in concrete pavements occurred in many cases after many years of service at loads below the static ultimate strength of the slab.

The Illinois test, as reported by Clemmer (6) and Older (28, 29), was devised to simulate the loading on the corner of the pavement slab, the most critical loading case. The test machine held 7 modulus of rupture beams cantilevered from a central hub and blocks were fitted between the beams to complete a circular track. The load was applied by rubber-tired wheels revolving around the central hub at a rate corresponding to 40 load applications per minute. The load at failure of the fatigued beams was compared with static ultimate strengths of companion beams.

Four series of beams were tested in this investigation. As beams failed, additional beams were installed in the test machine; thus it was possible to compare beams with various loading histories. In this study the following conclusions were made:

- The endurance limit of concrete in flexure is between 51-54 percent of the static failure stress.
- The repeated application of load less than 50 percent of the modulus of rupture increases the strength of the concrete at the stressed section.
- The number of cycles to failure increases with the richness of mix and decreases rapidly with increases of stress above 50 percent of the modulus of rupture.

The fatigue tests of Hatt and Crepps conducted at Purdue were also motivated by the interest in highway pavement failures (14, 24). In Hatt's opinion the Illinois test's rate of loading was too fast and that absence of rest periods did not duplicate actual highway conditions. The Purdue tests had complete reversals of stress applied at 10 cycles per minute; tests were shut down overnight and on weekends to provide rest periods. The fatigue strength of fatigue specimens was compared to unfatigued companion modulus of rupture beams.

The results of the Purdue tests (27) indicated:

- No definite fatigue limit between 40-60 percent of the modulus of rupture for 28-day specimens.
- A fatigue limit between 50-55 percent of the modulus of rupture for 4-month specimens.
- A fatigue limit of 54-55 percent of the modulus of rupture for specimens over 6 months.
- A recovery of stiffness for overnight rest periods.
- Stressing a specimen below its endurance limit strengthened the member.

The next significant study of the fatigue of plain concrete was reported by Kesler in 1953 (18). Since fatigue investigations are time consuming by their very nature, Kesler wanted to determine the effect of speed of testing on the flexural fatigue life of plain concrete. The specimens used were 64 inches long, supported on a span of 60 inches, and loaded at one-third points. Two different compressive strengths of concrete (3600 and 4600 psi) were tested at rates of 70, 230, and 440 cycles per minute. The average S-N curves (stress versus log number of cycles of load) for all beams tested, regardless of strength or speed of testing, were very close together indicating that for the range of 70 to 440 cpm the speed of testing has a negligible effect. This finding is important since time can be saved by conducting the fatigue tests at higher speeds. Even though these tests were conducted to a maximum of 10 million cycles, there was no indication that an endurance limit exists for plain concrete.

During 1954-56 Kesler conducted flexural fatigue tests which studied the effect of range of stress on fatigue life (25). The specimens Kesler used were 6 in. x 6 in. x 64 in., supported on a span of 60 in., and loaded at the one-third points. Four series were tested with the ratio, R, of minimum applied stress to maximum applied stress varying from 0.13 to 0.75. The tests indicated as R increases, the value of the fatigue strength, at 10 million cycles, also increases from 56 percent of the modulus of rupture for R = 0.0 up to 85 percent of the modulus of rupture for R = 0.75. Again a fatigue limit could not be established.

Another investigation conducted by Kesler, as reported by Hilsdorf and Kesler in 1966, was much more comprehensive (15). In Kesler's

opinion, previous studies with loads applied between constant minimum and maximum values and no rest periods did not represent actual loading conditions. This investigation was conducted in two phases. Phase one of the investigation studied the effect a rest period had on fatigue life. Each specimen was loaded 4500 cycles and then rested for a period of either 1, 5, 10, 20, or 27 minutes; during the rest period the minimum load was maintained. It was shown that rest periods increased the fatigue strength of plain concrete. This effect was more noticeable for specimens which required a greater number of cycles to failure. The fatigue strength increased with increasing length of rest period, up to 5 minutes; for tests having rest periods of 5, 10, 20, or 27 minutes further increases in fatigue strength were negligible.

Phase two of this investigation, which consisted of two parts, studied the effect of variable loading on the flexural fatigue life of plain concrete. In part one, the maximum stress level was changed only once during the test. In part two, the maximum stress level was changed periodically between two stress levels. It was determined that the sequence of the applied loads affects the fatigue strength of concrete. A relatively low number of cycles at high loads increased the fatigue strength of concrete which was subsequently loaded at a lower load as compared to the strength of a specimen which had not been previously loaded. As the load was changed periodically between two stress levels, it was determined the fatigue life decreased with increased higher stress and also with increased number of cycles at the higher stress.

A commonly used theory of cumulative damage of concrete structures under repeated loads, known as the Miner rule, was checked and found to give unconservative values of fatigue strength at high loads and overly conservative values for low loads. A procedure was presented by Hilsdorf and Kesler to adjust the Miner rule so it could be safely used for design.

In 1972, Ballinger (4) conducted a two phase fatigue study which was similar to Kesler's 1966 investigation. One series of tests was conducted in which the load was applied between a set maximum and minimum load; the level of load was not varied during the test. In the second series of tests, specimens were subjected to two different levels of cyclic loads; the level of load was changed just once during the test. Ballinger's tests indicate the initial portion of the S-N line is not straight, it curves downward from 100% to intersect the linear portion. This low-cycle region exists up to about 70 cycles and it was Ballinger's opinion factors other than simple fatigue affect failure in this range of stress. Ballinger's other conclusions differed somewhat from those of Kesler. Based on the results of this investigation, Ballinger concluded that Miner's rule adequately reflects cumulative damage effects and that the order in which cyclic loads of different magnitudes are applied has no effect on fatigue life.

Effects of Entrained Air

There are basically four sources of air voids present in the cement paste of unhardened concrete: (1) air originally present in the inter-granular spaces in the cement and aggregate; (2) air originally present

within the particles of cement and aggregate but expelled from the particles before hardening of the concrete by inward movement of water under hydraulic and capillary potential; (3) air originally dissolved in the mixing water; and (4) air which is in-folded and mechanically enveloped within the concrete during mixing and placing. These are the only sources of air voids in concrete, whether or not an air-entraining agent is used (23).

Two terms are used to distinguish between the types of air voids found in concrete. The first term is "natural" or "entrapped" air. Neither of these terms is appropriate because there is no evidence of an air content which is naturally occurring in concrete and all air is entrapped in concrete paste, just by different mechanisms. However, these terms will be used simply because of their wide usage. Entrapped air is typically characterized as 1 mm or more in diameter and has a irregular shape because the void follows the contour of the surrounding aggregate particles. Entrapped air is randomly distributed throughout the concrete mass.

The second term used to describe air voids is "entrained" air. A better term may be "purposefully entrained air," since an air-entraining (sudsing) agent is added to the concrete to increase the number of air voids. The air voids are typically spherical in shape, between 10 and 1000 microns in diameter, and well-dispersed throughout the concrete mass. The primary purpose for using air entrained concrete in highway pavements is to improve its resistance to freeze-thaw action. The well-distributed air bubbles serve as reservoirs that accommodate expansion resulting from

the freezing of water within the concrete. As the freezing of water within the capillaries progresses, the expansion pressure is relieved by forcing the excess water into the air voids, thus the expansion during freezing can occur without fracturing the concrete.

Air entrainment also improves the workability of concrete. The air bubbles increase the spacing of solids in the concrete and allow easier movement of aggregate particles past one another. Air entrainment decreases segregation and bleeding by supplying a buoyant action to the cement and aggregate, by decreasing the area otherwise available for movement of water and solids, and by developing capillary forces between the air bubbles which slow the drainage of mixing water.

One adverse effect of air entrainment is the reduction in strength of the concrete. For a concrete containing 6 sacks of cement per cubic yard, each percentage increase in the amount of air above the entrapped air content reduces the flexural strength 2-3%. For concrete containing more than 6 sacks per cubic yard, the reduction in strength is somewhat larger while for leaner mixes the reduction is somewhat less.

There have been very few investigations of the effect of air content on the fatigue of plain concrete. A study conducted at Purdue University during the mid-1950's compared the fatigue behavior of nonair-entrained concrete and air-entrained concrete cylinders in compression (3). After testing 80 cylinders in fatigue, it was concluded that the fatigue behavior of nonair-entrained plain concrete and air-entrained plain concrete were not significantly different. This study investigated the fatigue behavior of concrete in compression, however the failure of highway pave-

ments is essentially a flexural tensile failure. Thus utilizing information from this study for concrete pavement behavior could lead to erroneous conclusions.

In 1977, a study conducted at Iowa State University investigated the flexural fatigue behavior of plain concrete (21). Five series of concrete beams were tested in which the only variable was air content. As a result of this investigation, it was determined that air content does affect the flexural fatigue strength of concrete; as air content is increased, flexural fatigue strength decreases.

Effects of Varying Water-Cement Ratios

One of the principal factors affecting the strength of concrete is the water-cement ratio; the strength increases as the water-cement ratio decreases. Concretes with higher water-cement ratios contain more water, which when it evaporates, leaves a greater number of voids, thus reducing the strength of the concrete. A general rule of thumb is the compressive strength of concrete will be raised approximately 5% for each 0.03 reduction in water-cement ratio.

In Kesler's investigation conducted during the early 1950's (18), concrete flexural specimens of different compressive strengths (3600 and 4600 psi) were tested. The fatigue behavior of the specimens of different strengths were not significantly different, therefore Kesler concluded that the compressive strength, and thus the water-cement ratio, had no effect on the flexural fatigue strength of plain concrete.

Reduction of the water-cement ratio increases the quantity of air-entraining agent necessary to produce a given air content, but the air content required for maximum resistance to freezing and thawing is decreased as the water-cement ratio is decreased.

Effects of Aggregate Type

The properties of the coarse aggregate in concrete play an important part in determining the stress at which cracks form; smooth gravel leads to cracking at lower stresses than rough and angular crushed rock (26). Flexural strength depends on the type of coarse aggregate used since the properties of the aggregate, especially the surface texture, affect the tensile strength. The effect of the surface texture on strength of concrete is more noticeable in high strength concrete, while the effect is nearly negligible in low strength concrete (2).

Bond between the aggregate and the cement paste matrix is due partially to the interlocking of the aggregate and cement paste and depends on the roughness of the aggregate. A rougher surface, such as provided by crushed limestone, results in a better bond; also better bond is usually obtained with softer, porous aggregates (26). In general hard, smooth surfaces which allow no penetration of moisture do not produce good bond. Bond is also affected by other physical and chemical properties of the aggregate.

When there is good bond the failure surface should contain some broken aggregate in addition to the more numerous particles which are pulled out from their sockets. An excess of fractured particles might

indicate that the aggregate is too weak. In high strength concrete the bond strength tends to be lower than the tensile strength of the cement paste so bond failure between the aggregate and the cement paste predominates.

The properties of aggregate have some influence on the strength of concrete since low strength aggregate may limit the strength of the concrete. Even when the aggregate strength is higher than the strength of the concrete, the actual stresses at the points of contact of the particles may exceed the nominally applied stress, causing fracture. A low strength of the coarse aggregate may be due to either a weakness of grains or else the grains of the aggregate may not be well-cemented together.

The type of coarse aggregate influences the strength of the concrete, but the influence varies and depends on the water-cement ratio of the mix. It has been found for water-cement ratios below 0.40, use of a crushed aggregate has increased the strength up to 38% as compared to when gravel was used. As the water-cement ratio increases, the influence of the aggregate decreases until at a water-cement ratio of 0.65 no difference in strength is observed (26). This is because the strength of the cement paste becomes the controlling factor.

It has been determined that as the modulus of elasticity of the aggregate increases, the modulus of elasticity of the concrete increases. Kaplan (16) determined the modulus of elasticity of the aggregate was the most important single property of the coarse aggregate affecting the flexural strength of concrete.

Rigid Pavement Design

The factors which must be considered in the design of concrete pavements are the effects of traffic, climate, subgrade conditions, and the properties of concrete (11, 33). Pavement designs have evolved from analytical equations, laboratory research, road tests, field surveys of actual pavement performance, and development of semi-empirical equations.

The first concrete pavement in the United States was built in Bellefontaine, Ohio, in 1892. The pavement, portions of which are still in service, was built on the courthouse square and had a special grid pattern designed to provide safe footing for the horses which were expected to use the pavement.

The first mile of rural highway pavement in the United States, built primarily for automobiles, was constructed in Wayne County, Michigan, in 1909. To check their design, the Detroit Public Works Department conducted one of the first road tests. A twenty foot pole fitted with a set of steel shod horseshoes on one end and a heavy iron-rimmed wheel mounted on the other was revolved around a circular track consisting of sections of brick, granite, creosote block, cedar block, and concrete. The report of this test stated, "the concrete section laid under the specifications of the commissioners of Wayne County, Michigan, showed by far the best resistance to the severe test to which pavements were put" (31).

In 1922 and 1923 the state of Illinois constructed the Bates Test Road (28) containing different materials and different designs to provide the Illinois Division of Highways with information on the best pavement type and design. In this test, World War I army trucks were driven over

the 63 test sections. Of the 22 brick, 17 asphalt, and 24 concrete sections tested, one brick, 3 asphalt, and 10 concrete sections satisfactorily withstood the imposed loads. Until 1922, most concrete pavements had been built with no joints and with a thickened center section in an attempt to stop the formation of longitudinal cracks which developed in most of the 16-foot to 18-foot wide pavements of that time. Results of this test led highway officials to use a longitudinal center joint to eliminate cracking. Results were also used by Older to develop an equation relating pavement thickness to traffic loading based on the theory of cantilever beams.

In the mid-1920's, H. M. Westergaard (34, 35) of the University of Illinois, published several theoretical papers concerned with determination of stresses and deflections in concrete pavements. In Westergaard's papers three loading cases were considered: load applied in the interior of the slab, at the free edge, and at corners. Westergaard presented equations for the determination of pavement stresses which included the effects of size of load, subgrade reaction, concrete thickness, and modulus of elasticity. These equations were used by engineers for many years for pavement thickness design.

The Bureau of Public Roads conducted tests on concrete pavements at Arlington, Virginia, during the early 1930's. In these tests, measurements of stresses, deflections, and subgrade pressures were made to check the Westergaard equations. As a result of these tests, slight modifications were made by Westergaard, Kelly, Spangler, and Pickett on the

original Westergaard equations to provide closer agreement with actual measurements (11).

By the 1940's it was common practice to construct pavements with thickened-edge cross sections (5,12). The Arlington tests showed thickened-edge cross sections gave a pavement in which the stresses in the slab were approimxately equal for all positions of the load (17). The cross section had a uniform thickness in the interior and an edge thickness of about 1.67 times the interior thickness; the edge thickness was reduced at a uniform rate in a distance of 2 to 2-1/2 feet.

One of the most comprehensive road tests was conducted by the American Association of State Highway Officials (AASHO, currently known as the American Association of State Highway and Transportation Officials, AASHTO) and was reported in 1962 (31). Concrete pavements were subjected to traffic loads in four major traffic loops and in a light traffic loop. A control loop was subjected to a variety of nontraffic tests. The three variables in the test pavements were pavement thickness, depth of subbase, and the presence or absence of distributed steel reinforcement. Each pavement test section was subjected to only one axle spacing and weight. The results of the AASHTO road test indicate:

- Thin subbases (3-4 in.) perform as well as thicker (6-9 in.) ones.
- Properly jointed plain pavements, where there is adequate load transfer across joints, perform as well as reinforced pavements.
- Concrete pavements provide dependable performance where slab thickness is determined by the Portland Cement Association (PCA) design procedure.

The PCA design procedure in use today (33) is based on theoretical analyses of concrete pavement behavior, model and full scale tests, full scale test roads which are loaded by controlled test traffic, and observations of pavements in normal service.

Current design methods recognize maximum concrete tensile stress as the controlling factor of pavement failure. As a result, flexural stresses and flexural strength are used by the PCA in its thickness design method. Modulus of rupture tests are used to determine the flexural strength.

A second major factor in the PCA pavement design method is the modulus of subgrade reaction, k. The k value is equal to the load in psi on a loaded area divided by the total deflection in inches for that load. The k value can be determined by field measurements, but since pavement thickness is relatively insensitive to small changes in k, it is sufficient to determine a range of k values. It is usually not economical to construct subbases to increase the k value, therefore, the naturally occurring modulus of subgrade reaction is used in pavement thickness design.

Early design methods included an impact factor of 10 to 20 percent. However, tests conducted during the Maryland Road Test indicated stresses at joint edges were 15 percent less at speeds of 40 mph than at creep speeds. When 3/4-inch boards were placed on the road to simulate joint faulting, the stresses were further decreased. These findings are expected since static loads must be applied for a period of time to produce

a maximum stress. The impact factors used today by the PCA are therefore really load safety factors (10).

Fatigue has long been recognized as a cause of failure of concrete pavements. The original 1933 PCA fatigue curve (8) was based on the results of the tests conducted at Illinois and Purdue. The present PCA fatigue curve was drawn to be conservative with respect to the curve which resulted from Hilsdorf and Kesler's study of varying fatigue loads (15). Hilsdorf and Kesler felt their research was too limited for general adoption of their results.

Since fatigue is a function of applied stresses and number of repetitions, traffic is a major factor in thickness design. The AASHTO Interim Design Procedure (1), which is used by many highway departments, converts traffic into the total number of equivalent 18 kip single axle loads applied during the design life of the pavement in its design procedure. The PCA design procedure (33), used by the Iowa Department of Transportation, considers the cumulative fatigue effects of heavy axle loads in its design procedure.

Since fatigue of concrete is recognized as an important factor in the design of concrete pavements, and since the original data, on which the pavement fatigue design curves are based, were collected in the mid-1920's, long before air-entrainment was universally used, factors which might influence the fatigue life of concrete pavement (19), especially those related to air-entrained concrete, should be studied in order to provide a more efficient and economical design of concrete pavements.

PURPOSE AND SCOPE

Rigid pavement design procedures currently in use consider the modulus of rupture strength of concrete in determining the fatigue life of pavement. One fatigue curve is used regardless of air content, water-cement ratio, or aggregate type used in the concrete. The original fatigue tests, on which pavement design curves have been based for the last 40 or 50 years, were conducted in the early 1920's by the Illinois Division of Highways long before the introduction and widespread use of air-entrained concrete pavements.

Concrete pavements today are made with different air contents, water-cement ratios, and aggregate types. In order to produce an efficient and economical design, one must know what effects these factors have on the flexural fatigue strength of concrete. A research project conducted at Iowa State University in 1977 (21), indicated air content affected the fatigue life of concrete. The purpose of this study is to determine the effects of varying air contents, varying water-cement ratios, and different aggregate types on the flexural fatigue strength of concrete and establish design curves to be used in rigid pavement design.

The scope of this study includes the flexural fatigue testing of ten series of plain concrete. All batches were prepared with one cement type. The variables include air contents, water-cement ratios, coarse aggregates, and fine aggregates. The various material combinations are best understood by consulting Table 1.

Table 1. Material, air content, and water-cement ratio combinations

Coarse aggregate	Gravel			Alden Limestone					
Fine aggregate	Hallett Sand			Hallett Sand			Bellevue Sand		
Air, % / W/C	2[a]	6	10	2[a]	6	10	2[a]	6	10
0.32				3.1-LH-32	5.9-LH-32	9.5-LH-32			
0.43	3.9-GH-43	6.9-GH-43	14.2-GH-43		6.7-LH-43			5.5-LB-43	
0.60				4.2-LH-60	6.2-LH-60				

[a]Non air-entrained

MATERIALS AND PROCEDURES

Testing Program

The objective of this study was to determine the effects of varying air contents, varying water-cement ratios, and different aggregate types on the flexural fatigue strength of concrete. The test program originally proposed was to study nine series. Two different water-cement ratios (low and high) with crushed limestone as the coarse aggregate and three levels of entrained air (low, normal, and high) comprised six series while a normal water-cement ratio with gravel as the coarse aggregate and three levels of entrained air (low, normal, and high) comprised the remaining three series. From previous work (21) it had been determined that three levels of air content would be sufficient to demonstrate the effect of air content on fatigue. A previous fatigue study conducted at Iowa State University (21) tested concrete made with limestone at a normal water-cement ratio involving air content as the only variable. Therefore, in this study, concrete made with river gravel at a water-cement ratio of 0.43 was tested in order to compare the effects of gravel versus limestone on the flexural fatigue strength. Concrete at a high water-cement ratio with a high air content was not considered to be a usable mix, thus this series was replaced with one made with a coarse, high quality sand to determine what effect fine aggregate had on fatigue strength. A tenth series was added to serve as a control to check the reproducibility of the previous ISU study (21). For the material combinations, see Table 1. Series designations are also given in Table 1. Each series has a three

part designation which includes in order the following: plastic air content, coarse and fine aggregates used, and water-cement ratio times one hundred. In the aggregate part, the two letters employed have the following meaning:

L = Crushed Limestone

G = Gravel

H = Hallett Sand

B = Bellevue Sand

The age variable was reduced by testing all series at an age of 28 to 56 days. This meant that one series was mixed and poured approximately once each month. After the initial 28-day period when the first series was being cured, fatigue testing proceeded continuously. The second series was poured when testing began on the first series. While the first series was being tested, the second series was being cured. At the end of the 28-day curing period for the second series, testing of the first series was completed, the third series was poured, and testing of the second series began. This cycle continued until testing of all ten series was completed.

Beams for fatigue testing were 6 in. x 6 in. x 36 in. A modulus of rupture test was performed on the first 18 in. of the beam (Figure 1A) and a fatigue test was performed on the remaining unstressed portion (Figure 1B). This technique provided a modulus of rupture value for each fatigue specimen thus eliminating beam to beam variations. After the modulus of rupture test, and prior to the fatigue test, each beam was sealed in a plastic bag to maintain a constant saturated moisture content. Previous

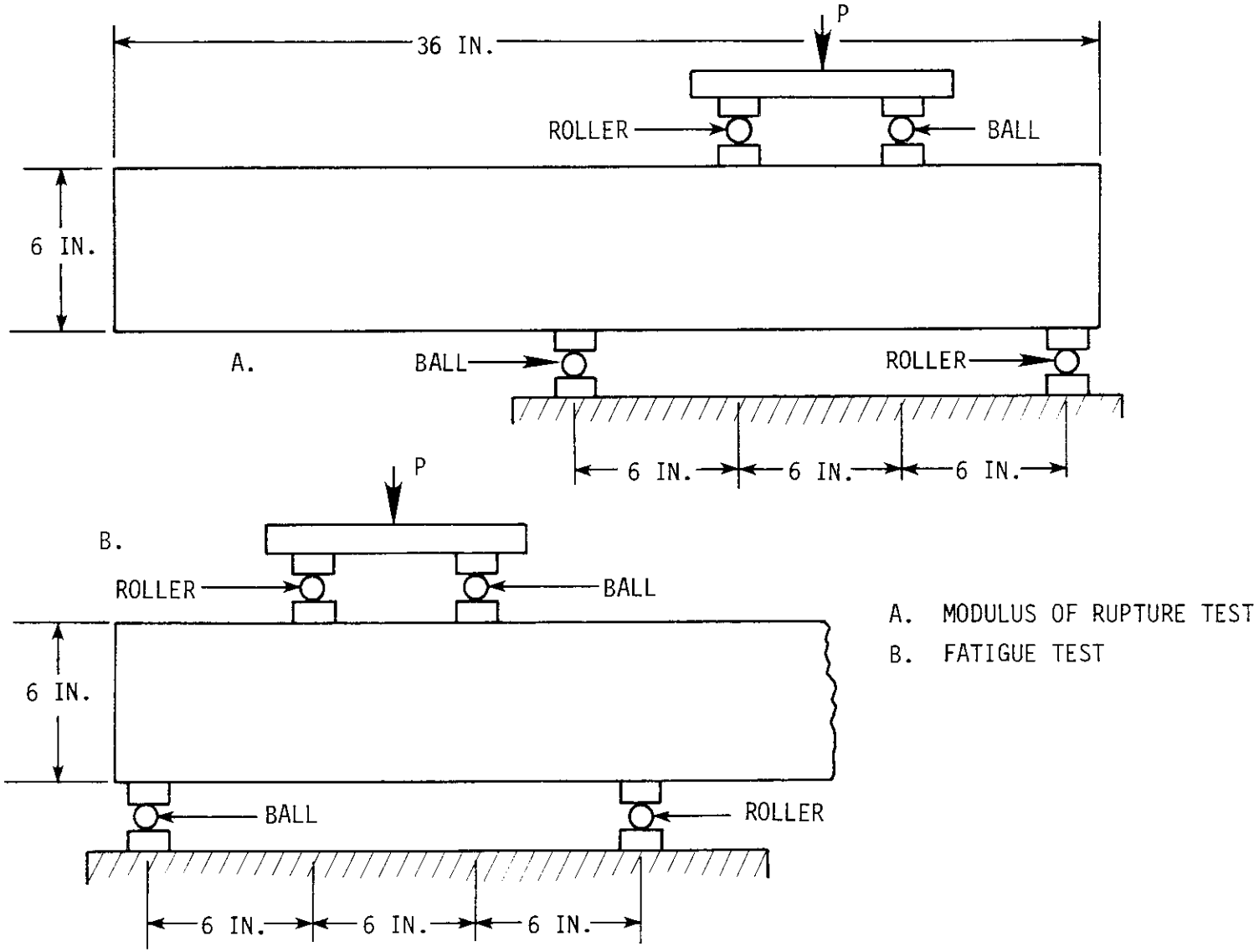

Figure 1. Schematic diagram of loading arrangements.

studies (30) indicate if specimens are allowed to air dry during fatigue testing, the scatter of data will increase. This is believed to be due to differential strains generated by moisture gradients within the beam.

The stress level for fatigue testing of each specimen was determined by taking a percentage of the modulus of rupture for that specimen. This stress level was then converted to an equivalent load to be applied to the beam. The equivalent load was applied to the beam until failure occurred. Load was varied from a nominal 100 pounds, which corresponds to less than 10 psi, to a maximum load corresponding to a predetermined percentage of the modulus of rupture stress. The bottom fiber was in tension throughout the test. Fatigue tests were conducted at four stress levels corresponding to 90%, 80%, 70%, and 60% of the modulus of rupture. Six specimens were tested at each stress level (20, 22). All tests in this investigation were run at a frequency of 5 hertz. As previously noted, Kesler (18) has shown that the speed of testing between 70 and 440 cycles per minute has a negligible effect on the fatigue strength of plain concrete.

In addition to the main fatigue test program, four other investigations were carried out. The subjects of the additional investigations are:

1) Modulus of rupture tests.

2) Compressive strength tests.

3) Determination of modulus of elasticity.

4) High pressure air tests.

Materials

The concrete used for the test specimens was a modified Iowa Department of Transportation (DOT) C-3 mix. A standard Iowa DOT C-3 mix contains a minimum of 604 pounds of cement per cubic yard and has a water-cement ratio of 0.43 (32). Since one of the variables studied was the water-cement ratio, it was necessary to change the cement content in order to produce a workable mix. Trial batches were run for each mix design to assure the proper air content and a slump between 1 and 3 inches.

Two types of coarse aggregates were used in this study. The gravel came from the Boggess Materials Company near Emmetsburg, Iowa, and had a saturated-surface-dry specific gravity of 2.68 and water absorption of 1.25%. The crushed limestone came from the Alden Quarry near Alden, Iowa, and had a saturated-surface-dry specific gravity of 2.53 and an absorption of 2.54%.

Two types of fine aggregates were used in this study. The Hallett sand, which came from the Hallett Construction Company, Ames, Iowa, was used in 9 out of 10 of the concrete pours. This sand had a saturated-surface-dry specific gravity of 2.64 and an absorption of 1.15%. Bellevue sand, from the Bellevue Sand Company near Bellevue, Iowa, was utilized in the remaining concrete pour. Use of this sand was suggested by engineers of the Iowa DOT. Bellevue sand is a coarse sand with a saturated-surface-dry specific gravity of 2.63 and a water absorption of 0.90%. All fine and coarse aggregates utilized in this investigation came from state approved stockpiles. For further information regarding aggregate gradation and specifications, see Tables A-1 and A-2 of Appendix A.

The Type I Portland cement used in the concrete batches was obtained from the Marquette Cement Corporation in Des Moines, Iowa. In order to guarantee uniformity, care was taken to assure all of the cement utilized was taken from one batch at the cement plant. Chemical and physical properties of the cement are given in Table A-3 of Appendix A.

Upon recommendation of the engineers at the Iowa DOT the air-entraining agent used in this investigation was Ad-Aire, a vinsol resin made by the Carter Waters Company of Kansas City, Missouri. Before each concrete pour, trial batches were run to determine the amount of air-entraining agent to be used to produce a specific air content.

A water reducing agent was used in the concretes with a water-cement ratio of 0.32 to produce a workable mix. Plastocrete 161, manufactured by the Sika Chemical Company of Lyndhurst, New Jersey, was the water reducer recommended by engineers of the Iowa DOT. Plastocrete 161 is a polymer-type, nonair-entraining, water-reducing, strength producing admixture which conforms to ASTM C 494 Type A (water-reducing admixture) (7).

Mixing Procedures and Quality Control

A total of ten series of fatigue specimens were poured. Prior to each pour, trial batches consisting of the desired aggregate and water-cement ratio were run to develop a mix with the desired air content and slump (9). Each pour consisted of approximately thirty 6-in. x 6-in. x 36-in. flexural fatigue beams and ten 6-in. diameter x 12-in. cylinders. Approximately 1.1 cubic yards of concrete were required for each series.

Since control and uniformity of the mix was of utmost importance, all mixing was done in the laboratory. At the beginning of the project all materials were obtained and stockpiled in the laboratory for use throughout the project. A mixer of one cubic yard capacity could not be located, so a concrete mixing truck was rented on the day of each pour. Before the batch quantities were charged into the mixer, the mixing drum was inspected to determine if it contained any left over concrete or mixing water from a previous job which would alter the desired mix. The batch quanities (see Table A-4 of Appendix A), which had previously been weighed out and corrected for moisture contents, were then charged into the empty concrete mixer. According to Iowa DOT specifications (32), the concrete was mixed 70 revolutions; at the end of such time, slump tests and plastic air content tests were run to check the acceptability of the concrete. If the concrete was acceptable, it was transferred to the beam forms by wheelbarrow. If the concrete was unacceptable, the batch was adjusted (keeping the water-cement ratio constant) until it fell within the acceptable limits. The beams were then vibrated according to ASTM C 192 (7) with a 1 in. diameter pencil vibrator which operated at 10,500 vibrations per minute. As the concrete was being placed in the beam forms, cylinders for compressive strength tests and modulus of elasticity tests were being cast in 6-in. diameter x 12-in. waxed cardboard cylinder molds with concrete that was representative of that in the beams.

The beams were then finished and covered with wet burlap and a heavy polyethylene sheet to maintain a moist condition for proper curing.

The burlap was kept wet and after a period of 48 to 72 hours, the forms were stripped and the beams were moved to large metal curing tanks where they were cured under water until they were tested.

The sequence from mixing to curing is shown in Figure 2.

The slump tests were run according to ASTM C 143 (7); air content tests were run according to ASTM C 231 (7). Three air meters of the pressure type from the Iowa DOT were used throughout the project. The air meters were calibrated prior to the beginning of the study and used exclusively in the study. For consistency, the same operators ran the air tests throughout the study.

Equipment

At the end of the 28 day curing period compression tests were run on the 6-in. diameter x 12-in. concrete cylinders using a 400,000 pound capacity Baldwin-Satec Universal Testing Machine. Modulus of elasticity tests were conducted on the same machine using a Tinius Olsen concrete cylinder compressometer following ASTM standard C 469 (7).

The modulus of rupture of each specimen was determined under one-third point loading utilizing a concrete beam tester, Model S6, made by the American Beam Tester Company.

For the fatigue testing, an Instron Model 1211 dynamic cycler was used. A load frame was constructed so that flexural one-third point loading, at the same spacing as the modulus of rupture test, could be applied. The Instron has a ±20,000 pound capacity and the load can be applied at a frequency of 5 to 35 hertz. Near the end of the study, a

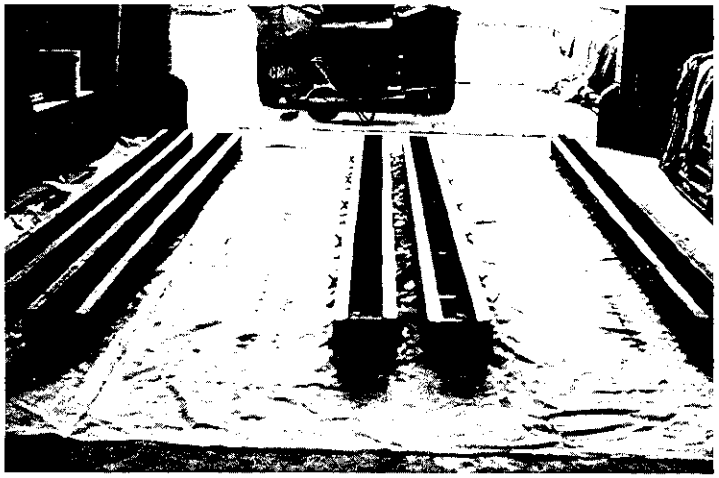

(a) Concrete mixing truck and empty forms.

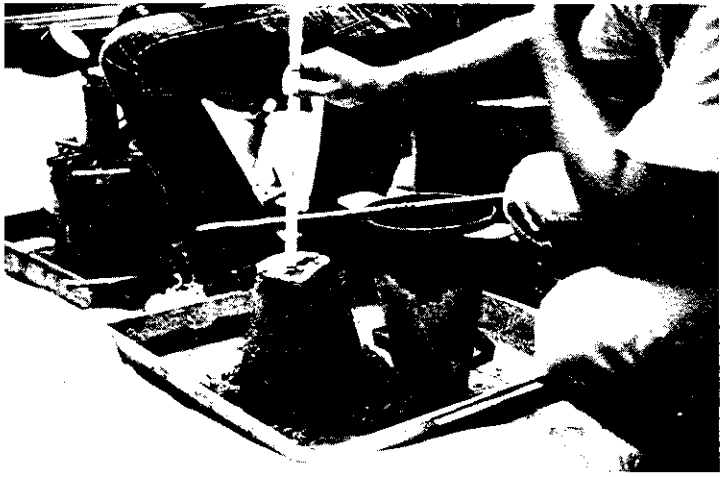

(b) Slump and air tests.

(c) Concrete forms being filled and vibrated.

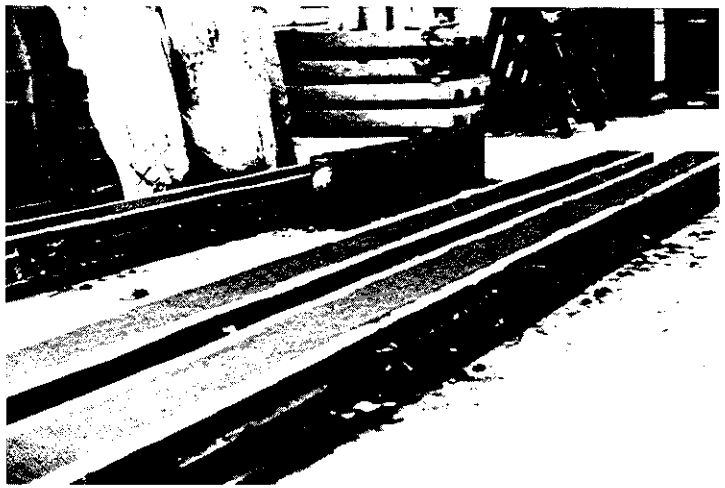

(d) Finished beams.

Figure 2. Sequence showing steps in preparing fatigue specimens.

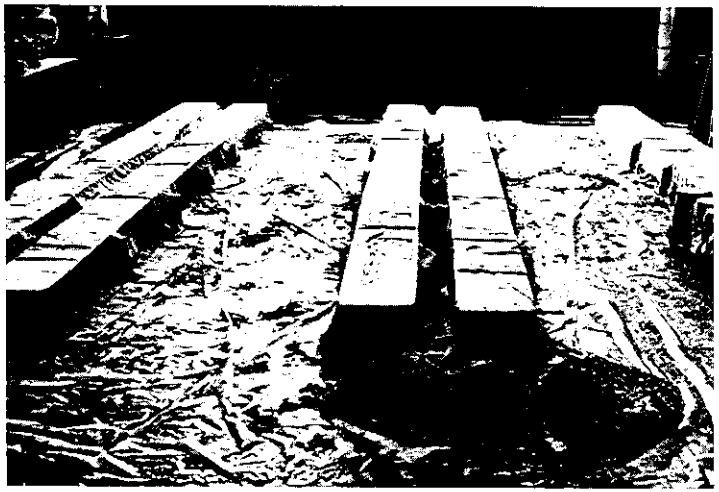

(e) Beams covered with wet burlap.

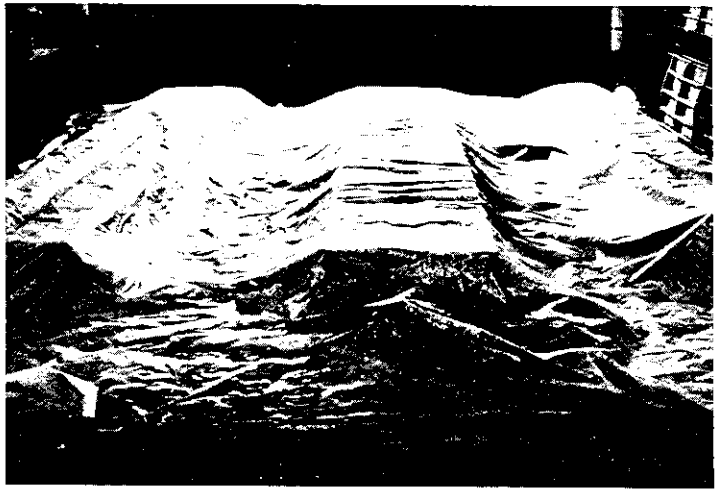

(f) Beams covered with polyethylene sheet.

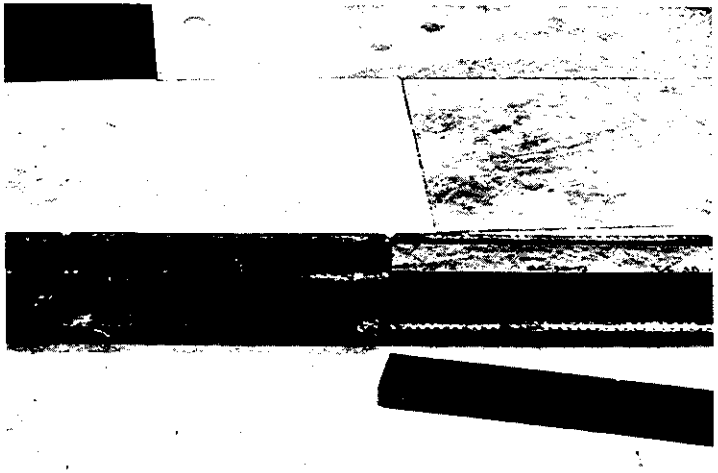

(g) Forms being stripped.

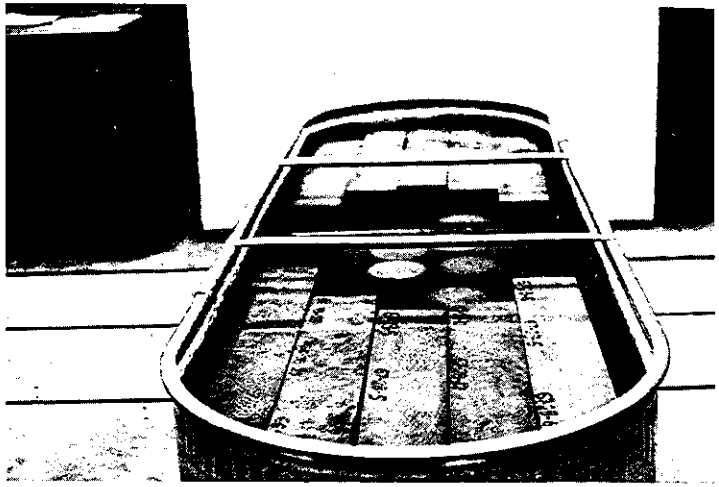

(h) Beams in curing tank.

Figure 2. (Continued). Sequence showing steps in preparing fatigue specimens.

Materials Test System, MTS, fatigue machine became available for use. It too had a load fixture constructed for applying flexural one-third point loading at the same spacing as the modulus of rupture machine. The MTS has a capacity of ±110,000 pounds and can apply the load at a frequency of .00001 to 990 hertz. Testing machines utilized in this study are shown in Figure 3.

During this investigation all of the machines were calibrated. Strain gages were attached to an aluminum beam which was loaded at one-third points in the same manner as the concrete test specimens. Strains due to static loading in the 400^{k} universal test machine, the beam tester, the Instron, and the MTS were measured using a Vishay strain indicator. For dynamic loading in the Instron and MTS, a Sanborn Model 850 Dynamic Recorder was used to record the loads. All loads delivered were within acceptable limits of the load setting.

The high pressure air content was determined by the Materials Laboratory of the Iowa Department of Transportation. Four-inch diameter cores were drilled from sections of tested fatigue beams, oven dried at 300°F for 72 hours, and then cooled for 3 hours. After weighing, the cores were soaked in water for 48 hours. The cores were then weighed in water, removed and patted dry with a cloth, and weighed again in air to determine absorption. The cores were placed in the high pressure air meter and pressure of approximately 5000 psi was applied. Air content was then computed from dial readings based on Boyle's law. For more details of the procedure see Test Method No. Iowa 407-A, April 1971, Iowa Department of Transportation, Materials Department.

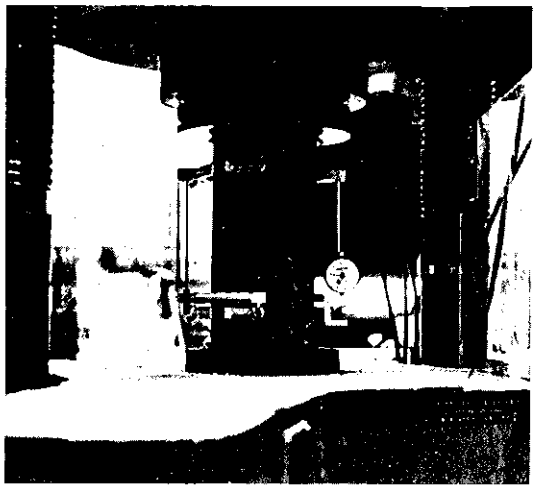

(a) 400^{k} machine with compressometer.

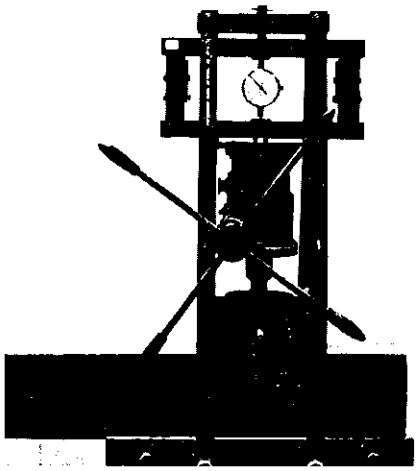

(b) Modulus of rupture machine with beam.

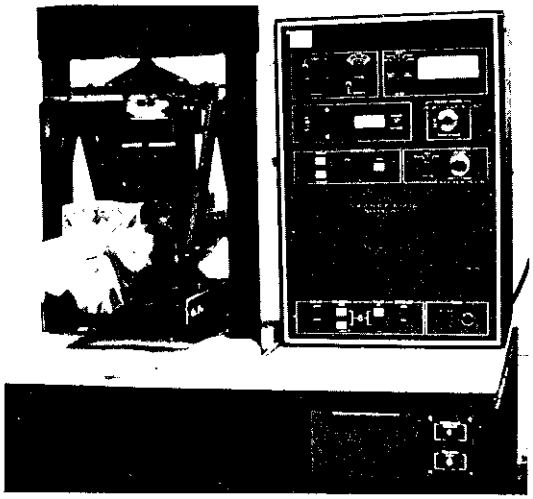

(c) Instron Dynamic cycler.

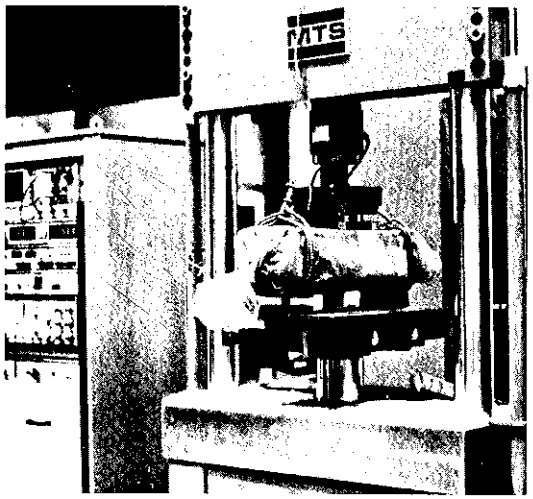

(d) MTS fatigue machine.

Figure 3. Test machines utilized.

RESULTS AND DISCUSSION

Physical Properties

Herein is presented the experimentally determined physical properties of the ten series of concrete tested in this study. A summary of the concrete properties for the various series is presented in Table 2. The modulus of elasticity is the average of three tests, the 28-day compressive strength is the average of four compression tests, and the modulus of rupture value is the average of all beams tested in each series. In this table and throughout the remainder of this report percent air refers to plastic air content unless otherwise stated.

Modulus of elasticity

The modulus of elasticity tests were made using a standard concrete cylinder compressometer with a dial gage attachment following the procedure given by ASTM C 469 (7). As can be seen in Figure 4, an increase in the amount of entrained air decreases the modulus of elasticity for Series LH-32 and Series GH-43. For Series LH-60 there is a slight increase. The equations of the lines in Figure 4 are:

Series LH-32

$E_c = -0.1791(PA) + 5.0877$

Correlation coefficient = -0.9988

Series GH-43

$E_c = -0.2301(PA) + 6.0506$

Correlation coefficient = -0.9787

Table 2. Summary of concrete properties

Series	Air content, %	Slump, in.	Unit weight, pcf	Modulus of rupture, psi	Compressive strength, psi	Modulus of elasticity, psi
3.1-LH-32	3.1	1	147.0	783	7375	$4.55\ (10)^6$
5.9-LH-32	5.9	1 1/2	144.6	660	6520	$4.00\ (10)^6$
9.5-LH-32	9.5	3 1/2	135.0	550	4300	$3.40\ (10)^6$
3.9-GH-43	3.9	1 3/4	149.0	840	5200	$4.95\ (10)^6$
6.9-GH-43	6.9	4 1/4	145.2	735	4730	$4.75\ (10)^6$
14.2-GH-43	14.2	5 3/4	136.0	430	1905	$2.70\ (10)^6$
6.7-LH-43	6.7	5 1/2	137.5	527	2966	$3.25\ (10)^6$
5.5-LB-43	5.5	2 1/2	142.8	664	5625	$4.10\ (10)^6$
4.2-LH-60	4.2	2	143.5	625	3880	$3.25\ (10)^6$
6.2-LH-60	6.2	2 1/2	140.8	570	3560	$3.35\ (10)^6$

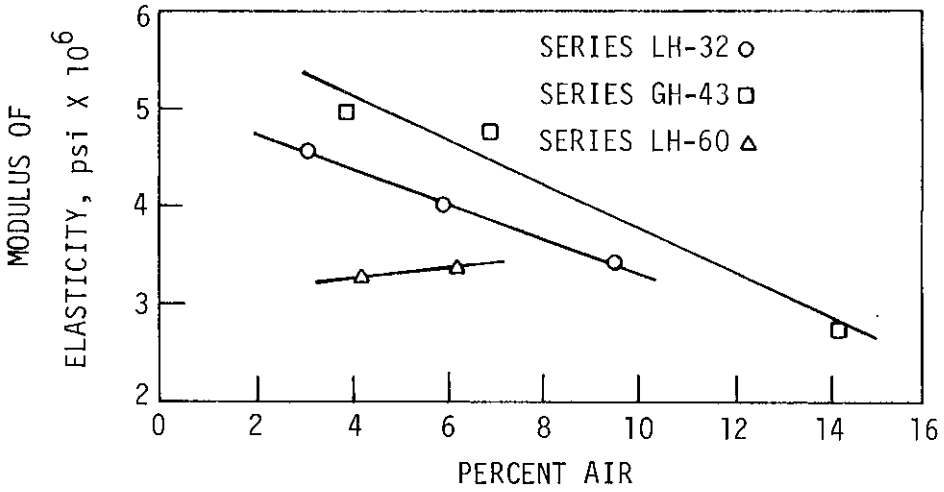

Figure 4. Modulus of elasticity versus percent air.

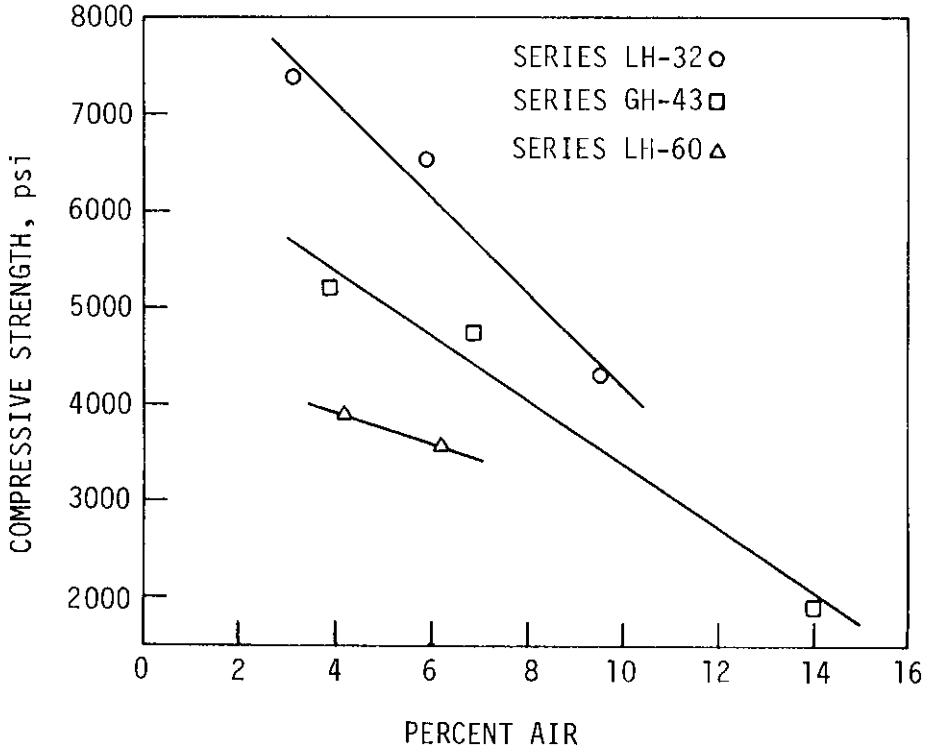

Figure 5. 28-day compressive strength versus percent air.

where

f'_c = 28-day compressive strength, psi

PA = plastic air content, percent

Modulus of rupture

The moduli of rupture, determined according to ASTM C 78-75 (7), were obtained from tests on one end of the fatigue specimens. Some previous fatigue studies determined an average modulus of rupture from testing a few specimens, and used the average modulus of rupture for all tests. However, in this investigation a companion modulus of rupture test was conducted for each fatigue specimen (see Figure 1), giving the most accurate estimate of the modulus of rupture. Also, the variation in strength due to age could be reduced since the modulus of rupture for each beam was determined at the time of the fatigue test.

The results of the modulus of rupture tests, as plotted in Figure 6, indicate that as the air content increases, the modulus of rupture decreases. For Series LH-32, GH-43, and LH-60, the modulus of rupture decreases approximately as the cubic root, square root, and fourth root of the percent air respectively. The equations of the curves according to a log-log regression analysis are:

Series LH-32

$$f_r = 1125.30(PA)^{-0.3126}$$

Correlation coefficient = -0.9945

Series GH-43

$$f_r = 1829.80(PA)^{-0.5279}$$

Correlation coefficient = -0.9647

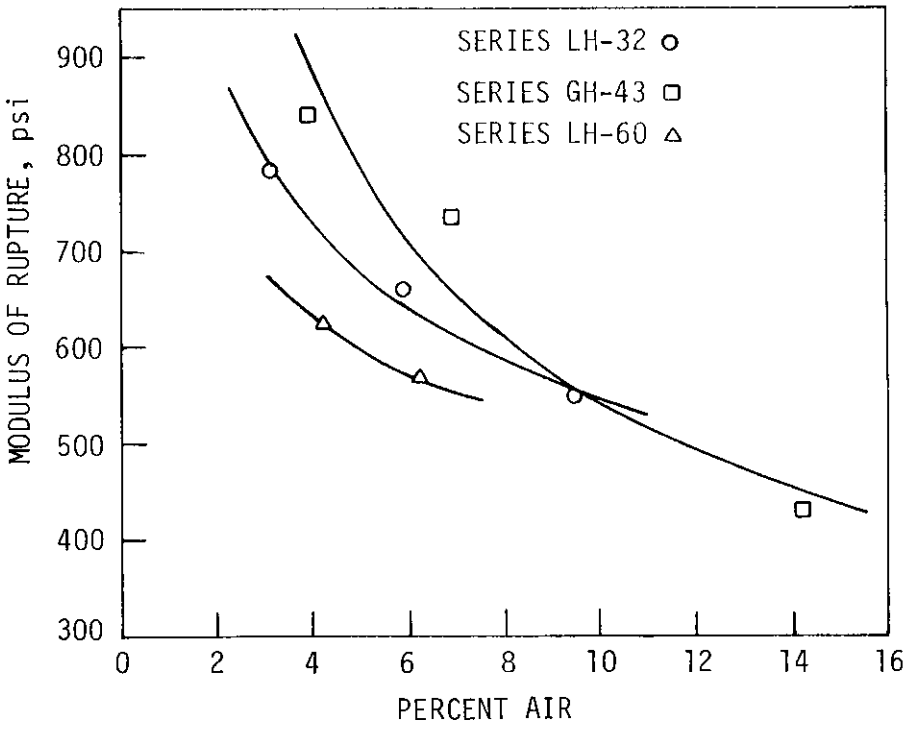

Figure 6. Modulus of rupture versus percent air.

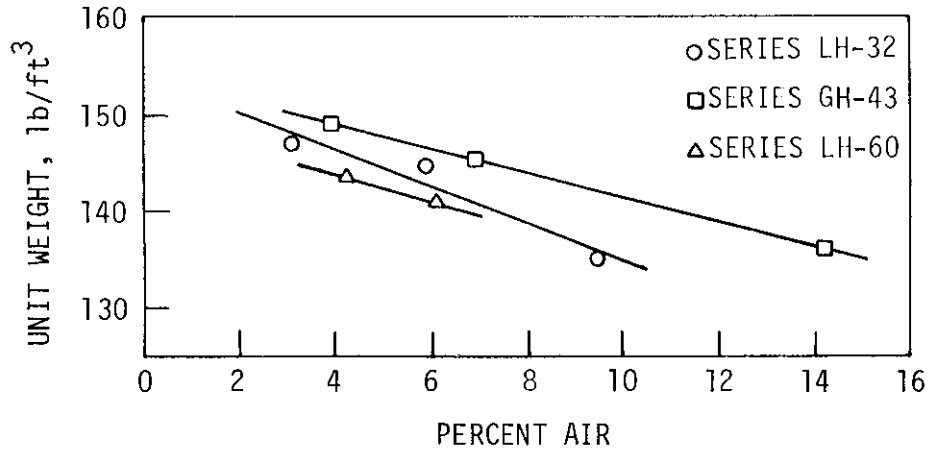

Figure 7. Unit weight versus percent air.

Series LH-60

$f_r = 877.59(PA)^{-0.2385}$

(No correlation coefficient is given as there are only 2 data points.)

where

f_r = modulus of rupture, psi

PA = plastic air content, percent

The modulus of rupture strengths in this investigation are probably somewhat higher than can be expected in the field due to the better control over the mix and the continuous curing until the time of the test.

Unit weight

At the time of the pour, the unit weight of each batch was determined. In each series, there is a linear decrease in weight of approximately 1-2 pcf for each percent air increase. A plot of the results is shown in Figure 7. The equations for the lines shown in Figure 7 are:

Series LH-32

$G = -1.9119(PA) + 153.9902$

Correlation coefficient, r, = -0.9660

Series GH-43

$G = -1.2618(PA) + 153.9149$

Correlation coefficient, r, = -0.9999

Series LH-60

$G = -1.3500(PA) + 149.1700$

(No correlation coefficient is given as there are only 2 data points.)

where

G = unit weight, pcf

PA = plastic air content, percent

Air Content

The air content used to compare the changes in modulus of elasticity, compressive strength, modulus of rupture, and unit weight was the plastic air content which was determined by the pressure method (ASTM C 231) (7). The air content of the hardened concrete was determined by the high pressure air method.

The results of the high pressure air tests are compared to the plastic air contents in Table 3. As may be noted, depending upon the series, the high pressure air content may be higher or lower than the plastic air content. The equation for the relationship is:

HA = .9968(PA) + 0.033

where

HA = high pressure air content, percent

PA = plastic air content, percent

Correlation coefficient = 0.9777

Fatigue Tests

The fatigue specimens were tested in flexure with the load applied at the one-third points, the same spacing as in the modulus of rupture tests. Ten different concretes were tested with various combinations of materials and levels of air content.

Table 3. Comparison of plastic air content and high pressure air content

Series	Plastic air content, %	High pressure air content, %			
		Individual tests			Average
3.1-LH-32	3.1	3.1	3.0	6.3	4.1
5.9-LH-32	5.9	6.0	6.7	6.1	6.3
9.5-LH-32	2.5	9.2	8.7	9.4	9.1
3.9-GH-43	3.9	-	-	-	-[a]
6.9-GH-43	6.9	5.9	6.4	5.4	5.9
14.2-GH-43	14.2	14.9	13.6	15.3	14.6
6.7-LH-43	6.7	7.1	7.1	6.9	7.0
5.5-LB-43	5.5	4.5	4.8	5.1	4.8
4.2-LH-60	4.2	3.0	4.6	3.2	3.6
6.2-LH-60	6.2	6.0	5.9	8.9	6.9

[a]Data not available.

The concrete test specimens within each series were tested at stress levels corresponding to 60, 70, 80, and 90 percent of the modulus of rupture. A minimum of five specimens, but more typically six specimens, were tested at each stress level for each series. A total of 239 flexural specimens were tested. The modulus of rupture strength, the maximum load applied as a percentage of modulus of rupture, and the fatigue life for each specimen are given in Tables B-1 through B-10 of Appendix B. As has been previously noted, each series has a three part designation. In Tables B-1 through B-10, there is a decimal point after the water-cement ratio. The number which comes after the water-cement ratio is the identification number of the individual beams within a given series. Specimens which did not fail are so indicated in these tables. In all but a few

cases, specimens which did not fail were loaded a minimum of 2 million cycles.

As stated before, the specimens were tested at 4 different stress levels. A constant minimum stress corresponding to less than 10 psi was maintained on the specimens so the bottom fiber was always in tension. Figure 8 shows the failure surfaces of several test specimens comparing the failure surfaces at similar air contents when different coarse aggregates and water-cement ratios are used. A difference in failure surfaces may be seen between concretes made with different coarse aggregate types at similar air contents (Figure 8B) as well as between concretes with different air contents (Figures 8A, B, and C) using the same coarse aggregate. At similar air contents (Figure 8B) concrete made with limestone seems to fail through the aggregate while the concrete made with gravel tends to fail around the aggregate. This result is in agreement with the findings of other researchers in that an aggregate with a rougher surface texture provides a better bond between the aggregate particles and the cement paste (26).

Inspection of the failure surfaces for each aggregate types shows increasing numbers of failures around the aggregate, as compared to through the aggregate, as the air content is increased. This indicates that high percentages of air weaken the bond between the cement paste matrix and the aggregate.

The fatigue data have been plotted on S-N curves (S = stress vs. log N = number of cycles to failure) for each of the 10 series. The curves shown in Figures 9 to 18 are the result of a log-log regression analysis

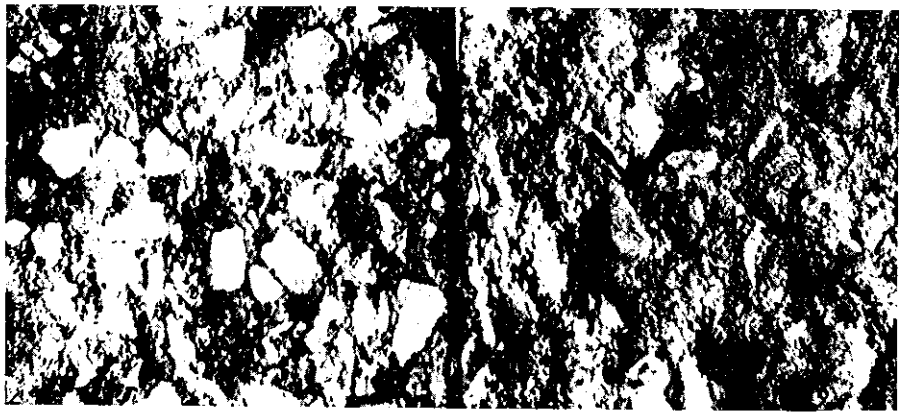

(a)

Series 9.5-LH-32 Series 14.2-GH-43

(b)

Series 6.7-LH-43 Series 6.9-GH-43

(c)

Series 3.1-LH-32 Series 3.9-GH-43

Figure 8. Failure surfaces of test specimens:
(a) high air content,
(b) medium air content,
(c) low air content.

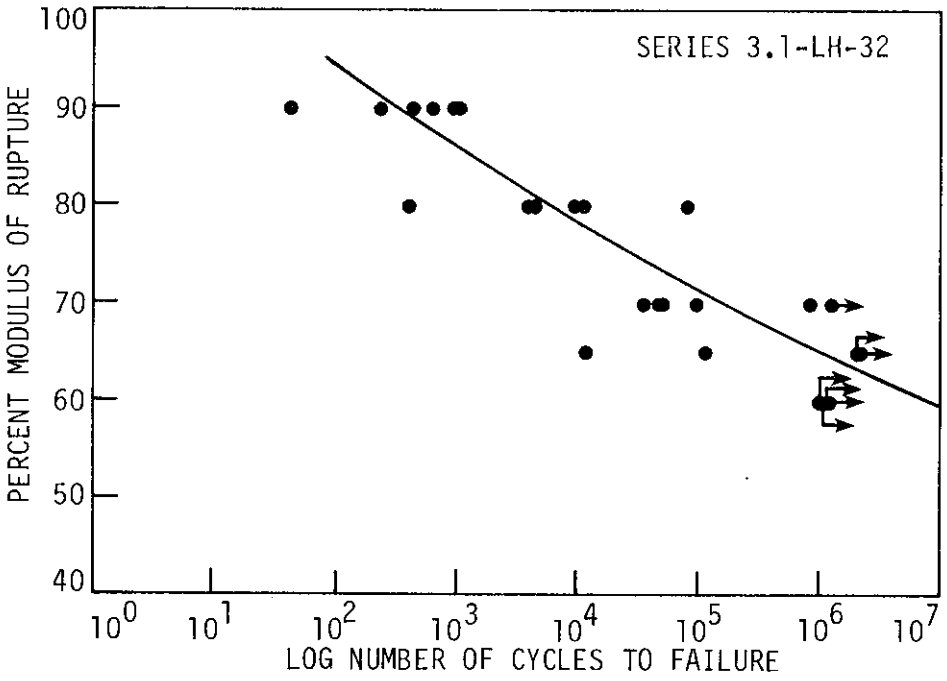

Figure 9. S-N curve for Series 3.1-LH-32.

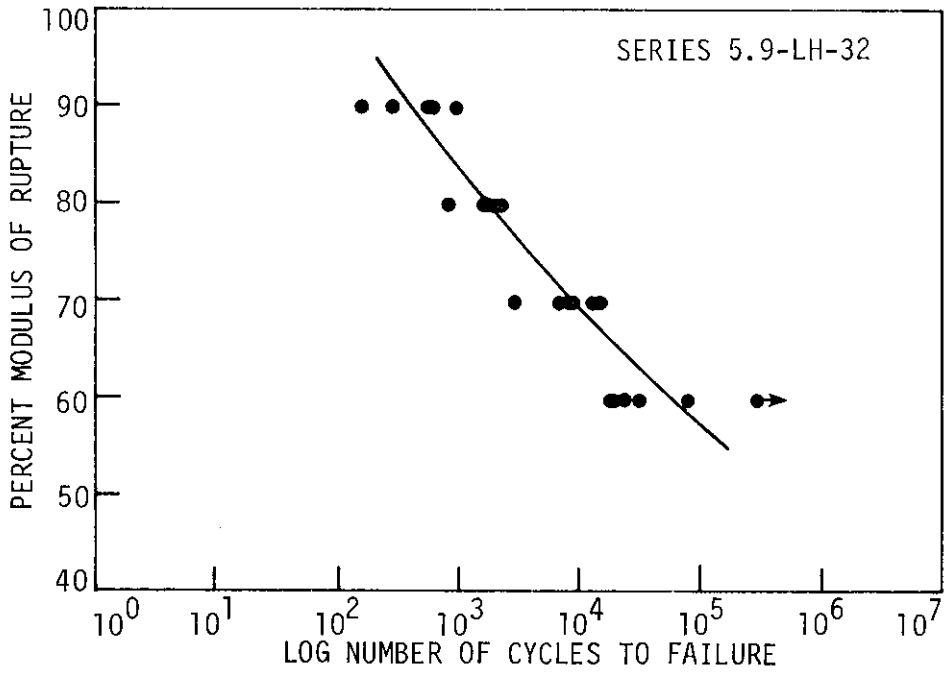

Figure 10. S-N curve for Series 5.9-LH-32.

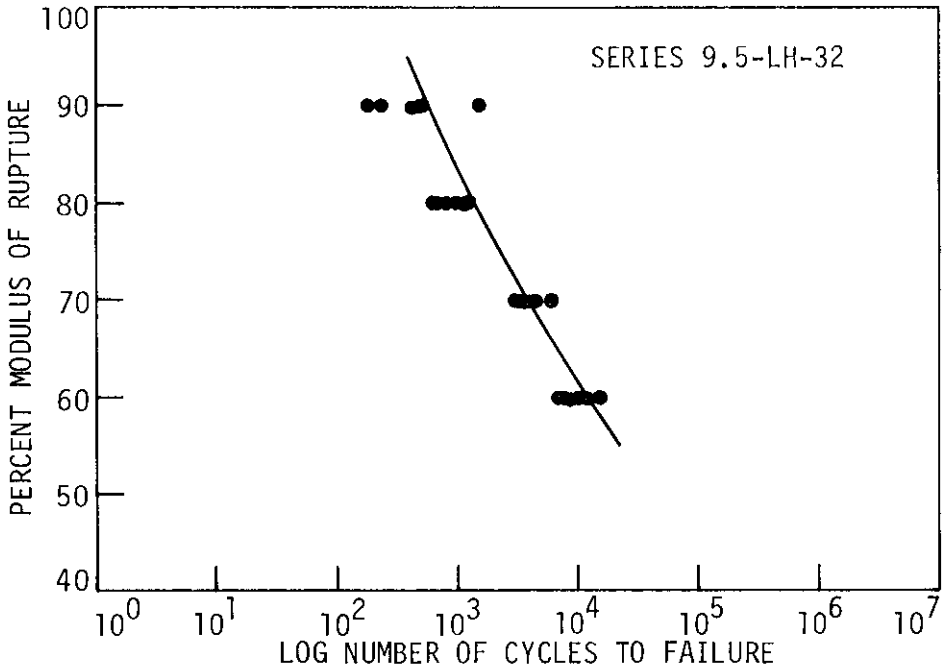

Figure 11. S-N curve for Series 9.5-LH-32.

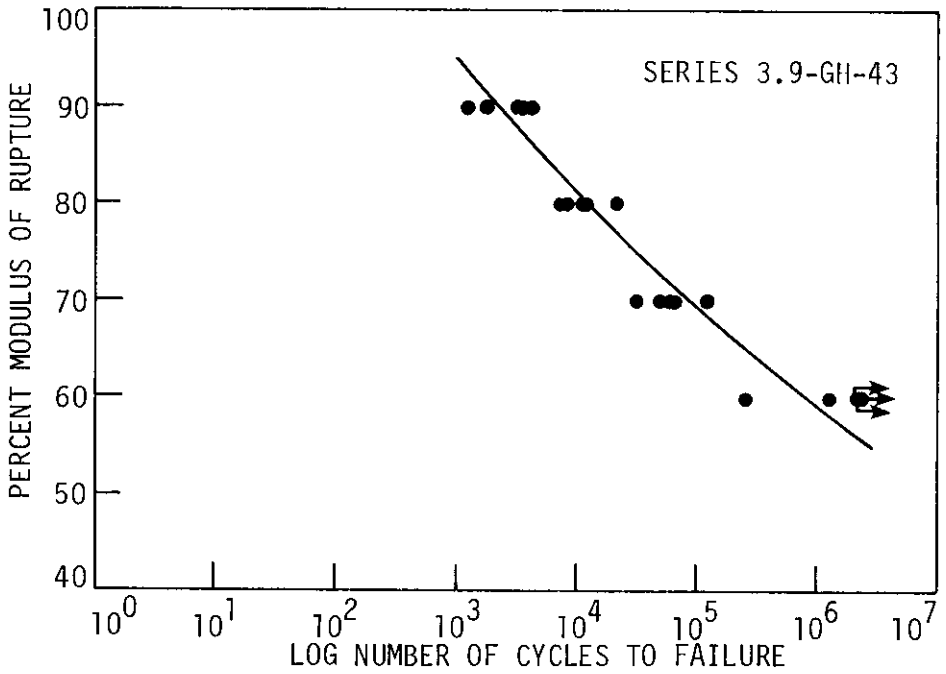

Figure 12. S-N curve for Series 3.9-GH-43.

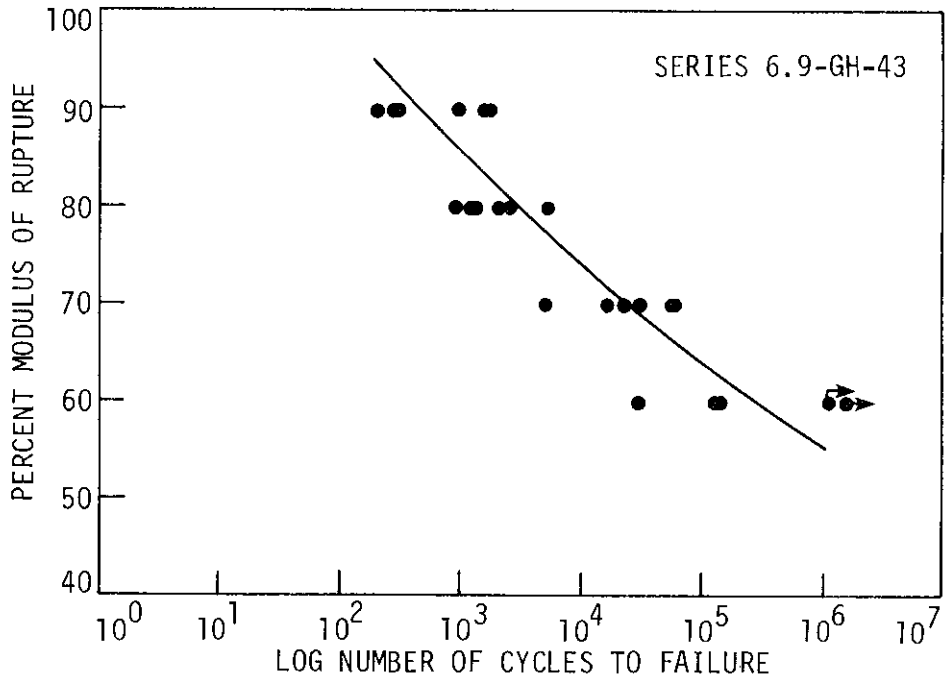

Figure 13. S-N curve for Series 6.9-GH-43.

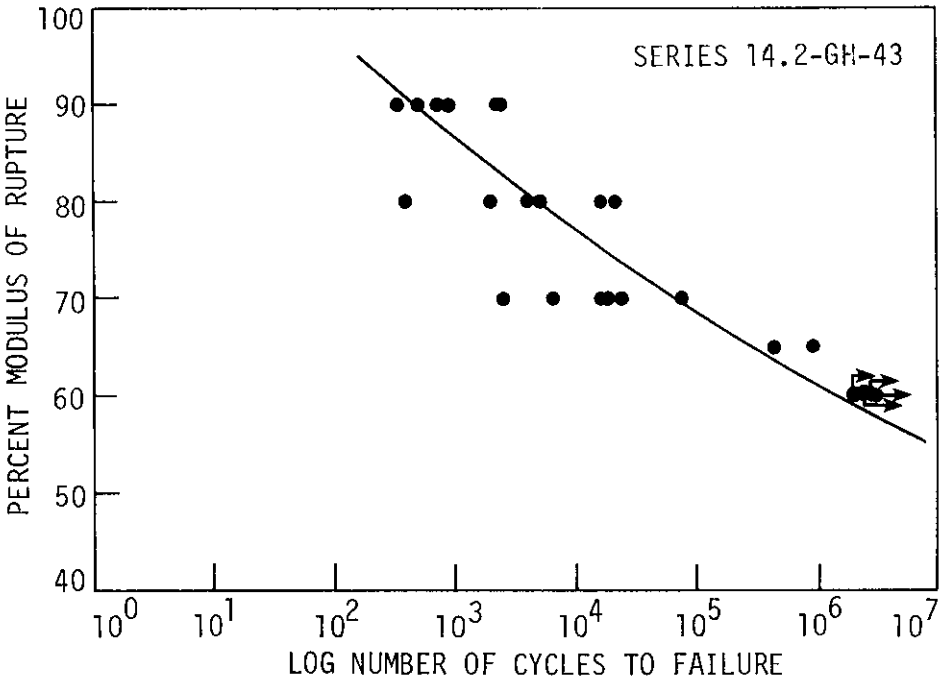

Figure 14. S-N curve for Series 14.2-GH-43.

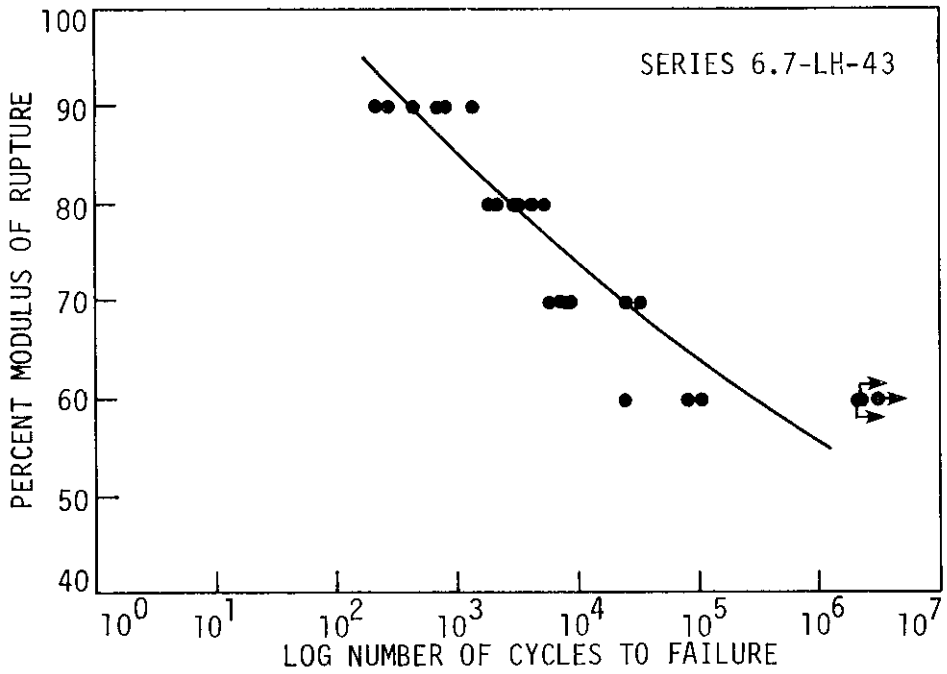

Figure 15. S-N curve for Series 6.7-LH-43.

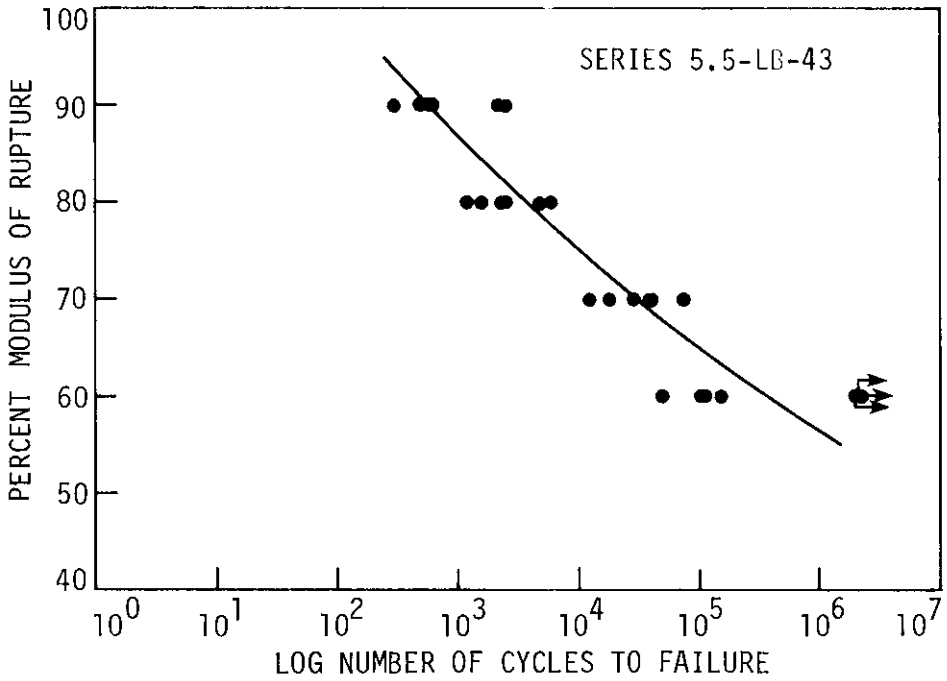

Figure 16. S-N curve for Series 5.5-LB-43.

program, CENSOR, which has the capability of considering and assigning values for the number of cycles to failure to specimens which did not fail. A discussion of the regression analysis of the data and the equations of the curves are given in Appendix C.

For comparison, curves representing concretes with identical water-cement ratios and aggregate types are shown in composite plots, Figures 19 to 22.

In the previous study conducted at Iowa State University (21) the only variable was air content. All concrete was made with Alden limestone, Hallett sand, and had a water-cement ratio of 0.41. This combination of materials, except for the slight difference in water-cement ratio, is essentially the same as Series LH-43 of this study. In order to provide a direct comparison of fatigue life of concretes made with gravel versus limestone at similar water-cement ratios as well as a comparison of fatigue life of concretes made with limestone at varying water-cement ratios, the basic fatigue data of the previous study (found in Appendix B of reference 21) was analyzed using the program CENSOR. The work of the previous study was renamed Series LH-41, to match the series designation of this report, and will be presented throughout the remainder of this report for comparison to the work conducted in this study.

The results of the log-log regression analysis for Series LH-41 are shown in Figures 23 to 27 and a composite plot is presented in Figure 28. Equations for the curves are given in Appendix C.

By studying the composite plots, Figures 19, 20, 21, 22, and 28 it is readily apparent that fatigue life decreases as air content increases,

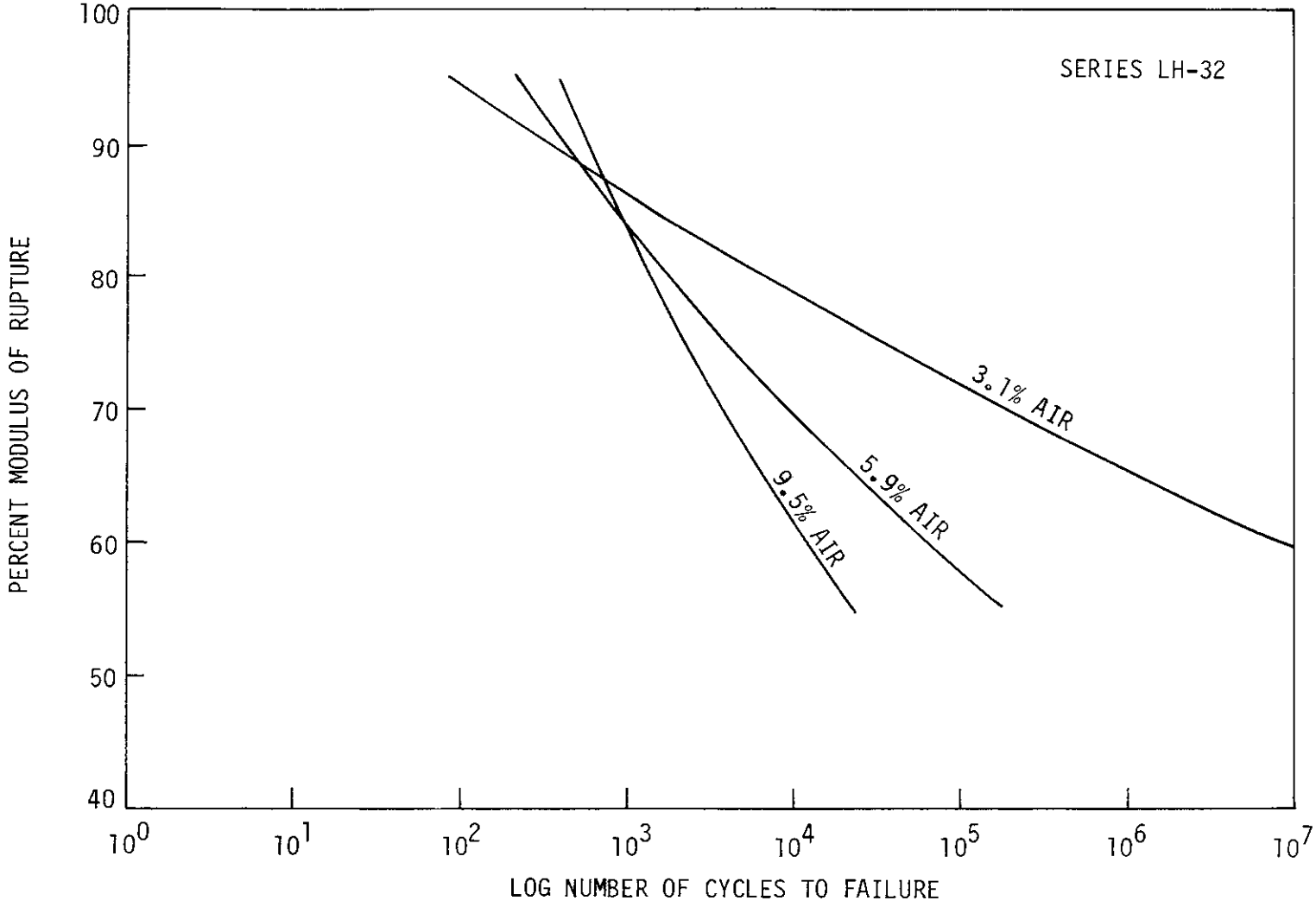

Figure 19. Composite S-N plot for Series LH-32.

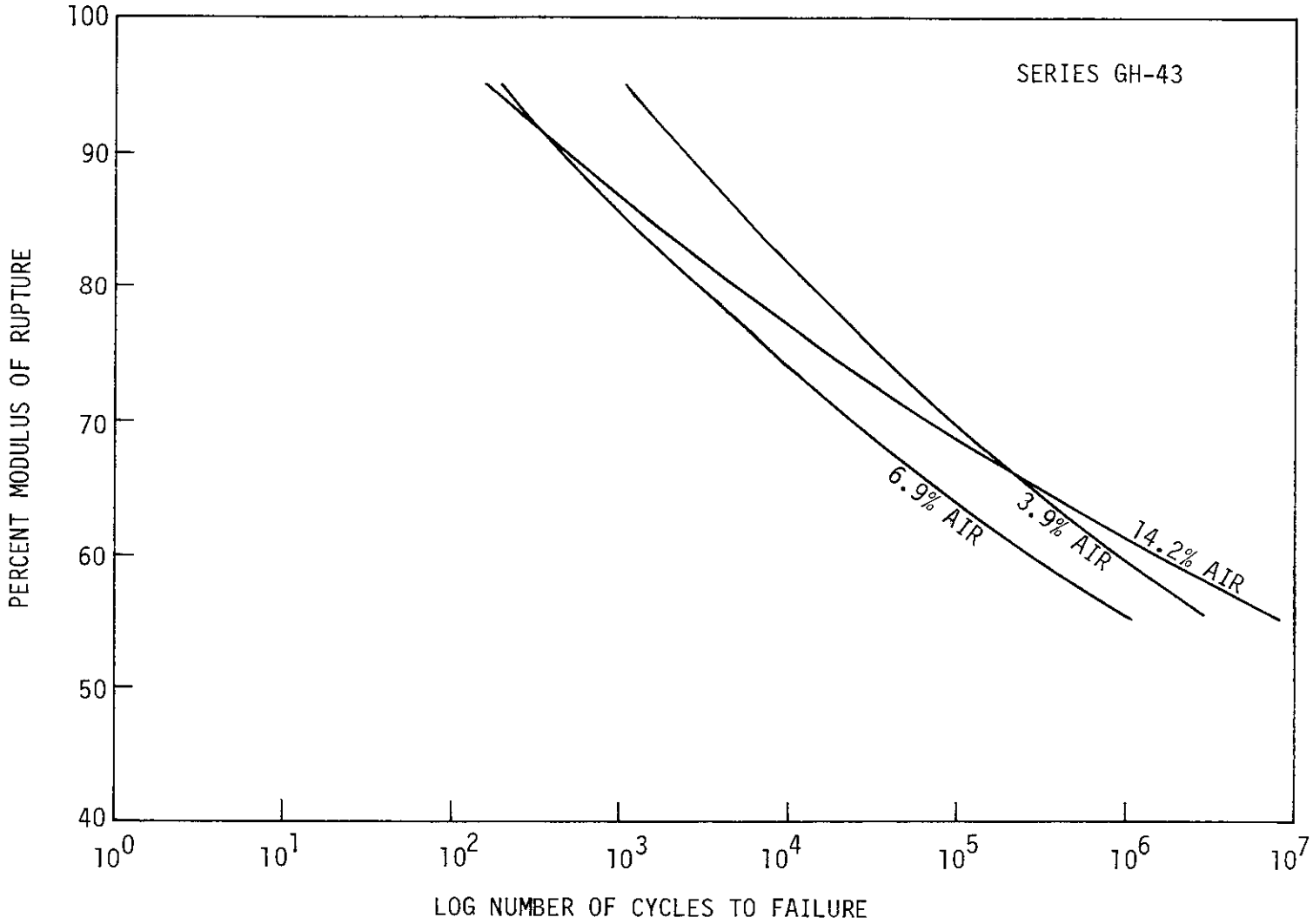

Figure 20. Composite S-N plot for Series GH-43.

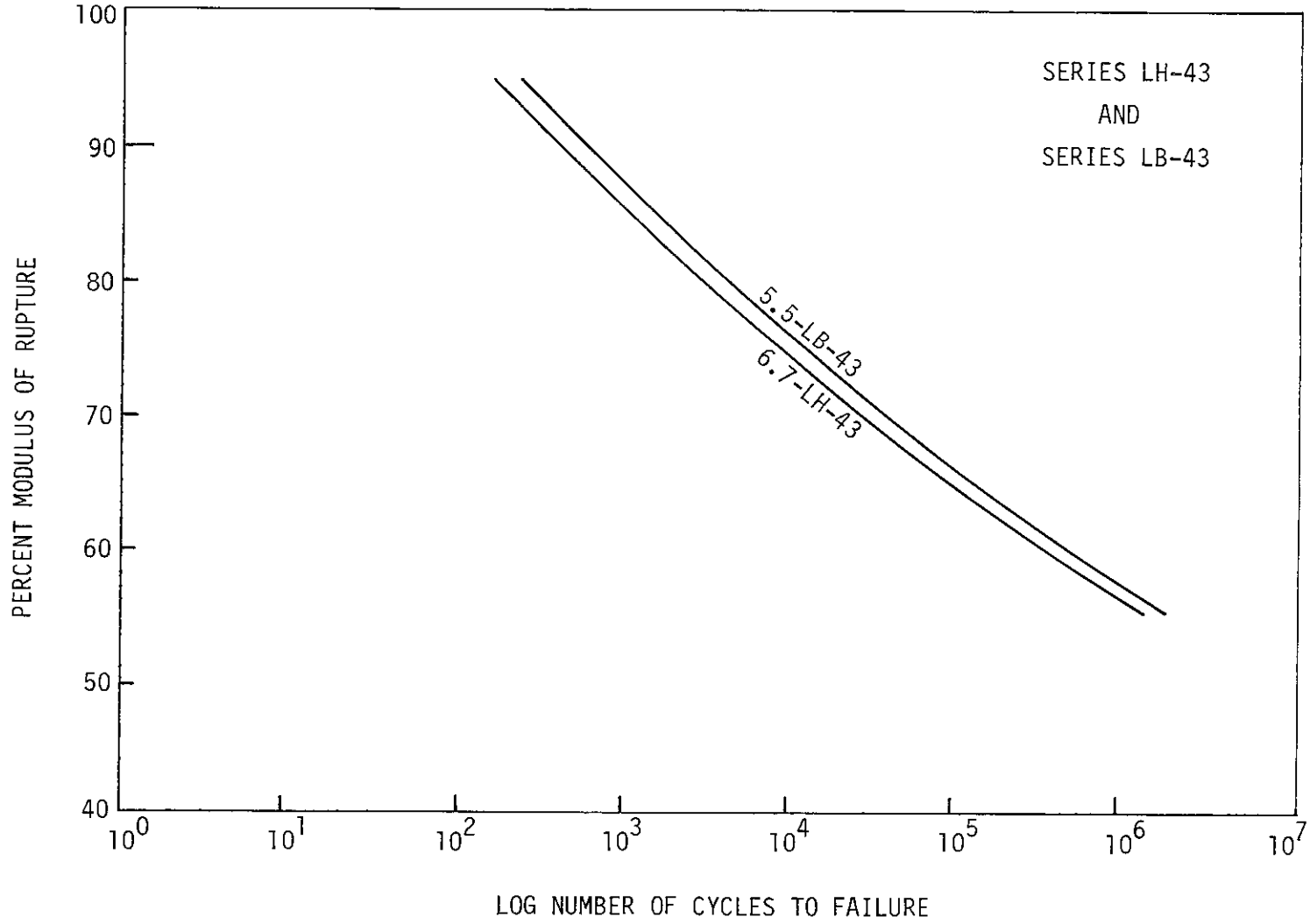

Figure 21. Composite S-N plot for Series LH-43 and Series LB-43.

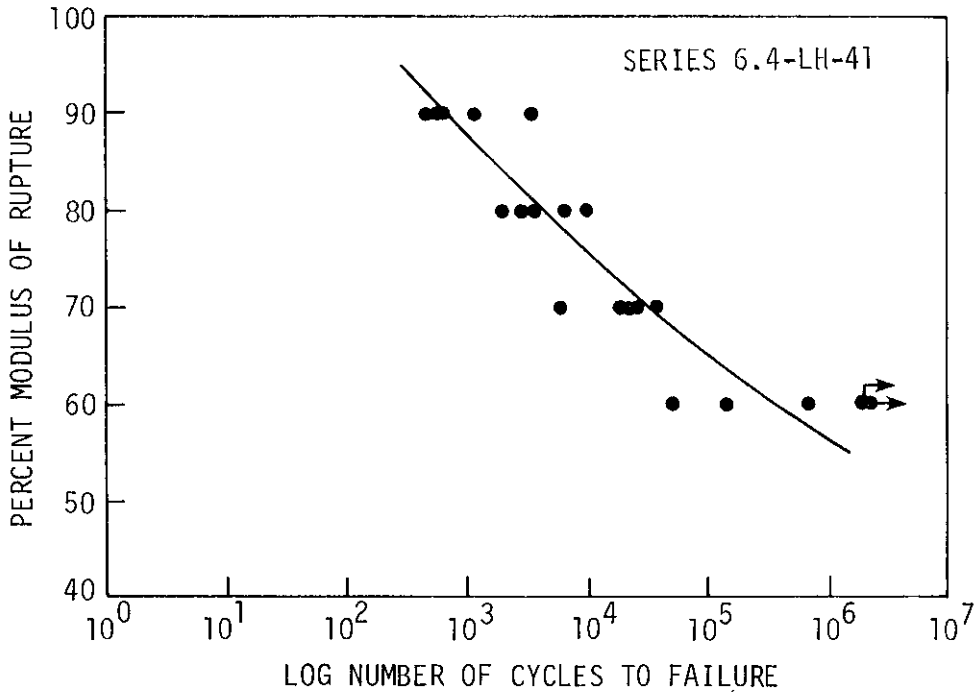

Figure 25. S-N curve for Series 6.4-LH-41.

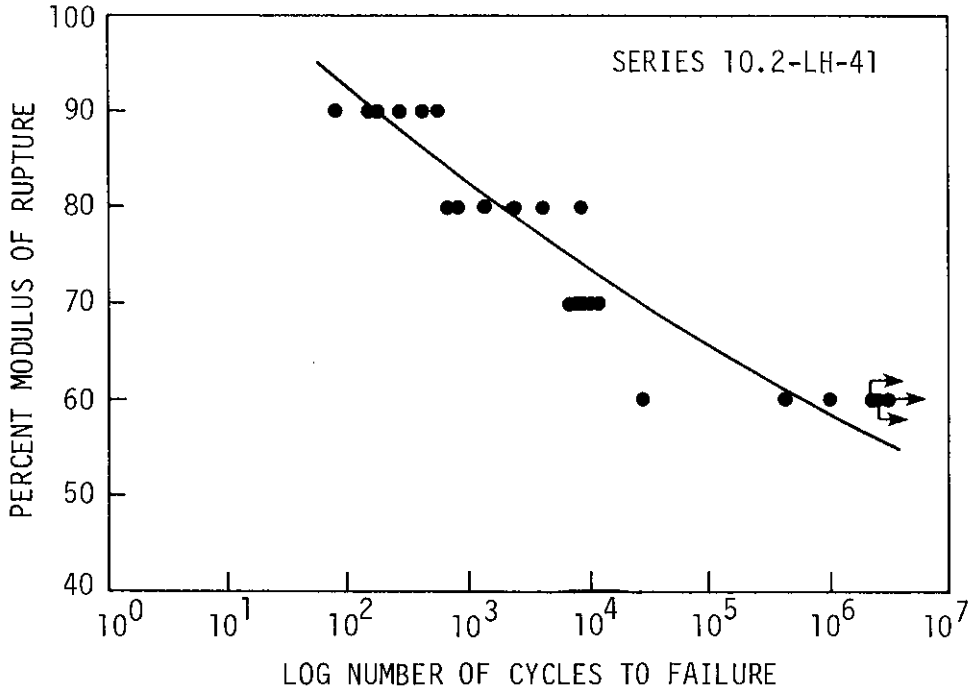

Figure 26. S-N curve for Series 10.2-LH-41.

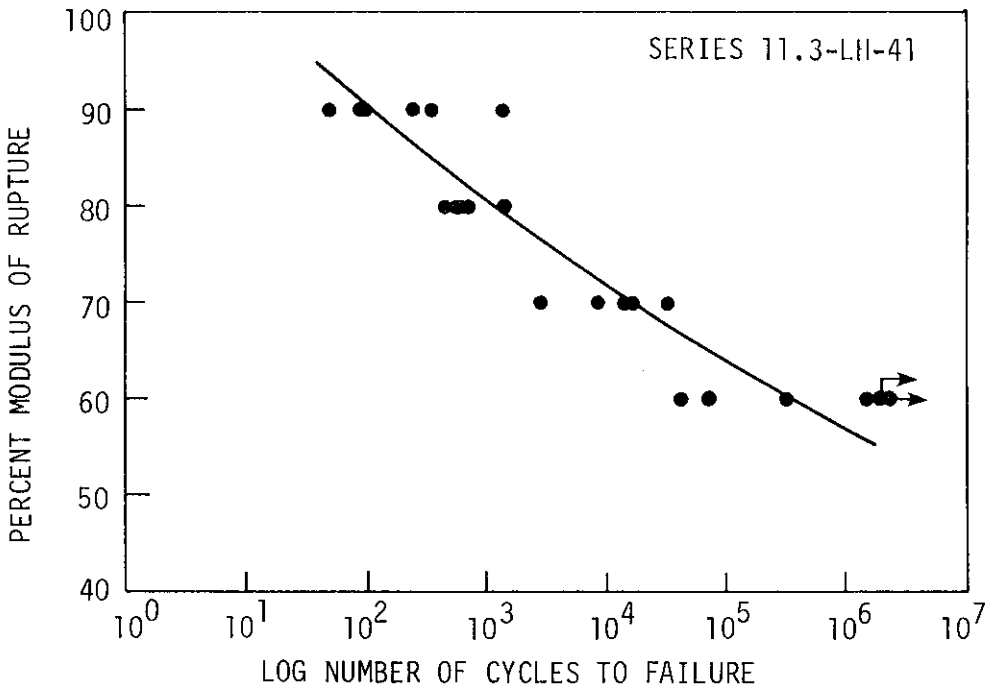

Figure 27. S-N curve for Series 11.3-LH-41.

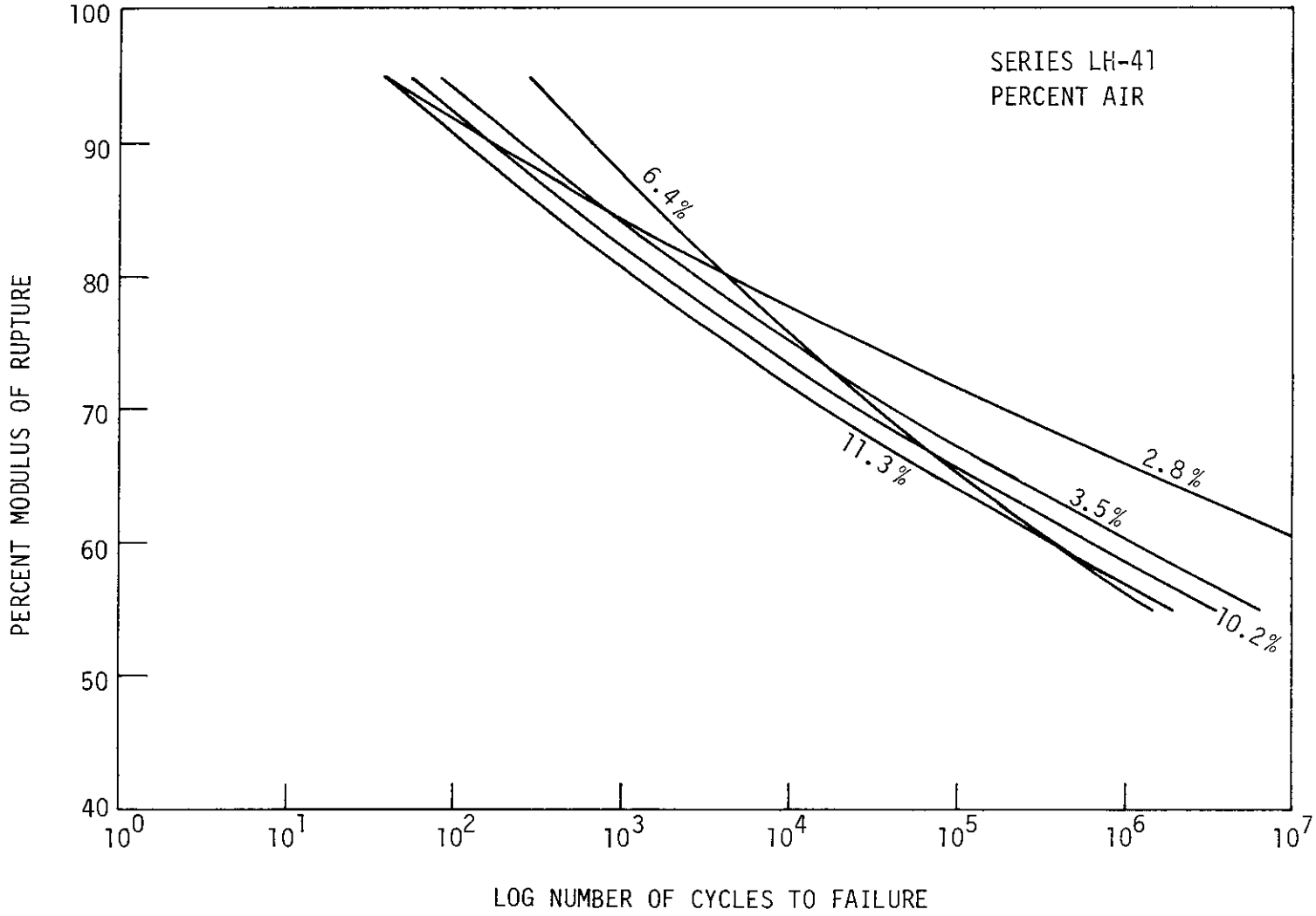

Figure 28. Composite S-N plot for Series LH-41.

regardless of the aggregate type or water-cement ratio. One exception to this general trend is the behavior of Series 14.2-GH-43 near the lower stress levels. Series 14.2-GH-43 had a high air content (14.2%) and a low modulus of rupture (430 psi). None of the specimens in Series 14.2-GH-43 failed when loaded at the 60% stress level; each of the unfailed specimens was loaded a minimum of 2 million cycles. This behavior and the method of analysis (CENSOR), in the opinion of the author, are the reasons for the fatigue curve found for Series 14.2-GH-43.

Comparing the composite plots, it can be seen that the curves diverge at the lower stress levels. The divergence may not appear to be significant on semi-log plots. However, in Series LH-32, Figure 19, at 70% of the modulus of rupture the difference between Series 9.5-LH-32 and Series 3.1-LH-32 is 171,000 while at 60% of the modulus of rupture the difference is 8,260,000. This divergence is important to pavement design since traffic normally causes stresses within these lower stress ranges.

There does not seem to be a general trend when comparing concretes with varying water-cement ratios, keeping the air contents and aggregate types constant. For low air content, the low water-cement ratio (0.32, Series 3.1-LH-32, Figure 9) produces a concrete with a higher fatigue strength than the medium water-cement ratio (0.41, Series 3.5-LH-41, Figure 24), and the high water-cement ratio (0.60, Series 4.2-LH-60, Figure 17). The concretes made with water cement ratios of 0.41 and 0.60 have similar fatigue strengths. For air contents around 6%, the low water-cement ratio (0.32, Series 5.9-LH-32, Figure 10) produces a concrete with a lower fatigue strength than the medium water-cement ratio concretes

(0.43, Series 6.7-LH-43, Figure 15, and 0.41, Series 6.4-LH-41, Figure 25) and the high water-cement ratio concrete (0.60, Series 6.2-LH-60, Figure 18). Again, the 0.43 and 0.60 water-cement ratio concretes produce fatigue curves that are practically incidental, indicating no difference in fatigue life. Thus, it may be concluded for water-cement ratios in the range of 0.40-0.60, the flexural fatigue strength is independent of compressive strength. For air contents around 10%, the low water-cement ratio (0.32, Series 9.5-LH-32, Figure 11) produces a concrete with a much lower fatigue strength than a concrete made with a water cement ratio of 0.41 (Series 10.2-LH-41, Figure 26). No series at a water-cement ratio of 0.60 at a high air content was tested.

At a water-cement ratio around 0.40 and at a low air content, the concrete made with gravel (Series 3.9-GH-43, Figure 12) exhibited a higher fatigue strength at the higher stress levels than the concrete made with limestone (Series 3.5-LH-41, Figure 24). At the lower stress levels there did not seem to be a significant difference in fatigue strength. At the water-cement ratio around 0.40 and at an air content around 6%, there was not a significant difference in the fatigue strength of the concrete made with gravel (Series 6.9-GH-43, Figure 13) versus that made with limestone (Series 6.7-LH-43, Figure 15, and Series 6.4-LH-41, Figure 25). At high air contents the concrete made with gravel (Series 14.2-GH-43, Figure 14) had a higher fatigue strength than the concretes made with limestone (Series 10.2-LH-41 and 11.3-LH-41, Figures 26 and 27).

The fatigue strength of Series 5.5-LB-43, Figure 16, the one series made with a high quality of fine aggregate, was not significantly differ-

ent from the fatigue strength of Series 6.7-LH-43 which was made at the same water-cement ratio and essentially the same air content but with Hallett concrete sand. There may be a slight increase in fatigue strength, although it is difficult to tell with the limited data available.

The reproducibility of the fatigue curves may be seen by comparing Series 6.9-LH-43, Figure 13 and Series 6.4-LH-41, Figure 25. Although there is a slight difference in the air content and water-cement ratio, the curves are essentially the same.

APPLICATIONS TO CONCRETE PAVEMENT DESIGN

The principal design considerations for the Portland cement concrete pavement thickness by the PCA procedure (33) are:

1. The pavement thickness is a function of the modulus of rupture of the concrete, the applied load, and the subgrade modulus k.
2. The fatigue failure in flexure is the key to thickness requirements and its effects are considered by the use of a linear summation of cycle ratios to account for mixed traffic loading and the cumulative fatigue damage (Minor's hypothesis).
3. The thickness design makes use of a general fatigue curve (or table) in which the ratio of applied stress to the modulus of rupture is related to the allowable number of stress applications.

The 1933 PCA fatigue curve (8) shown in Figures 34-37 is based on the research conducted by the Illinois Department of Highways and Purdue University in the early 1920's. This curve was used with Minor's hypothesis to estimate the accumulated fatigue damage in order to design a pavement of adequate thickness. Minor's hypothesis applies to stress repetitions above the endurance limit and postulates that fatigue strength not used by repetitions at one stress level is available for repetitions at other stress levels. The 1933 fatigue curve was replaced by the present 1966 curve, also shown in Figures 34-37, due in part to the work of Hilsdorf and Kesler (15) in the early 1960's, and, in part to theoretical analysis, full scale test roads, and observations of pavements in normal service.

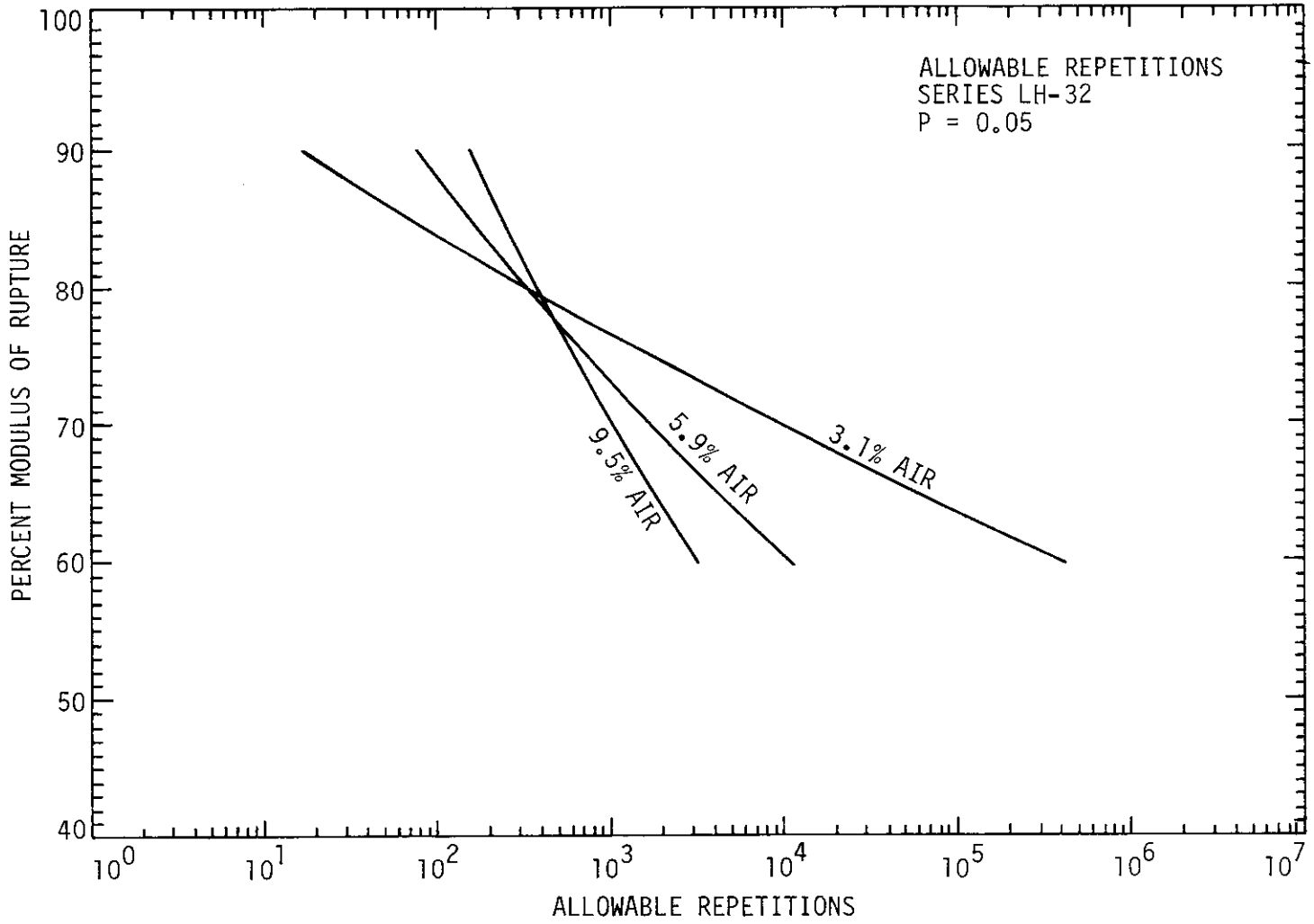

Figure 29. S-N curves showing allowable repetitions for Series LH-32.

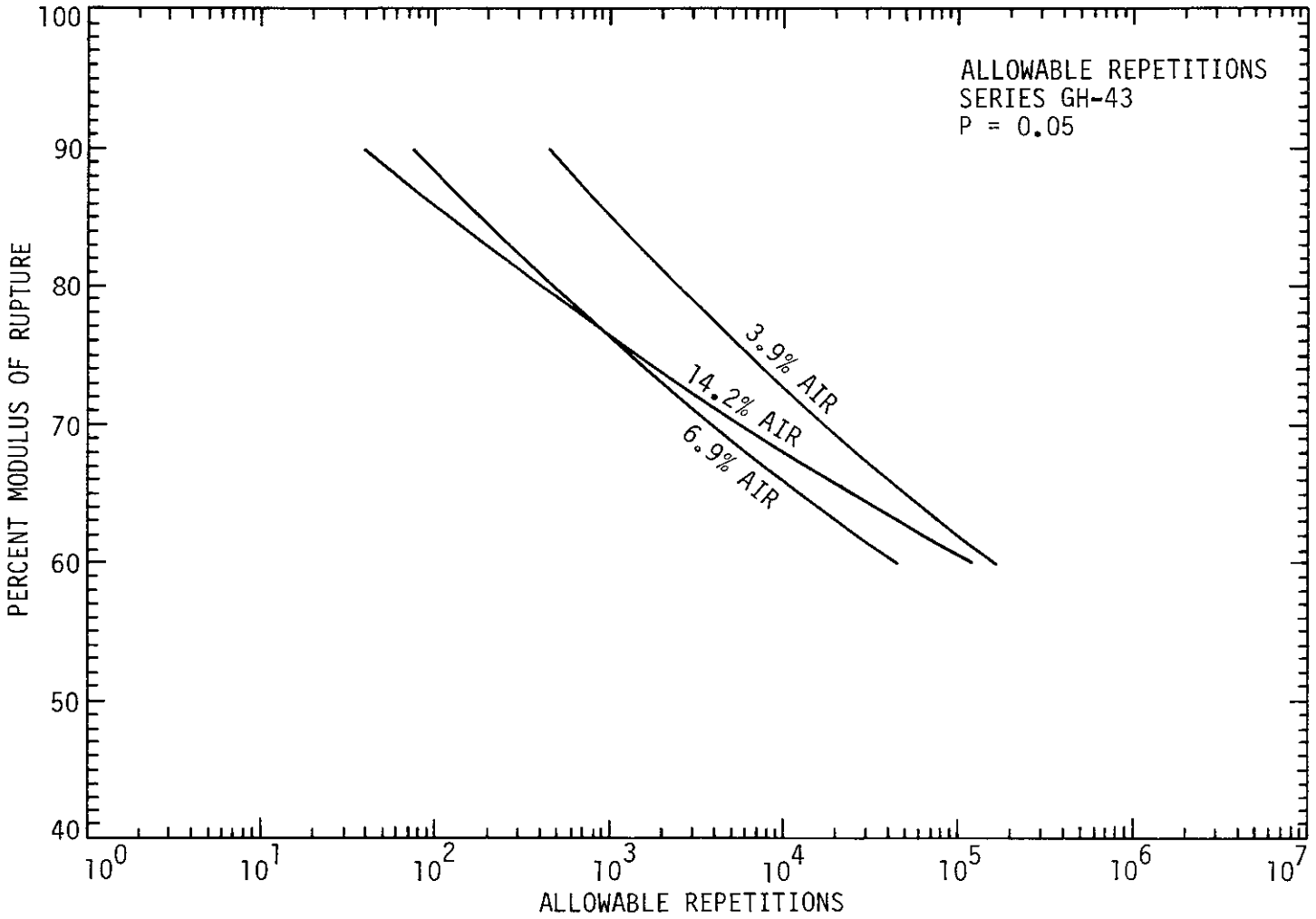

Figure 30. S-N curves showing allowable repetitions for Series GH-43.

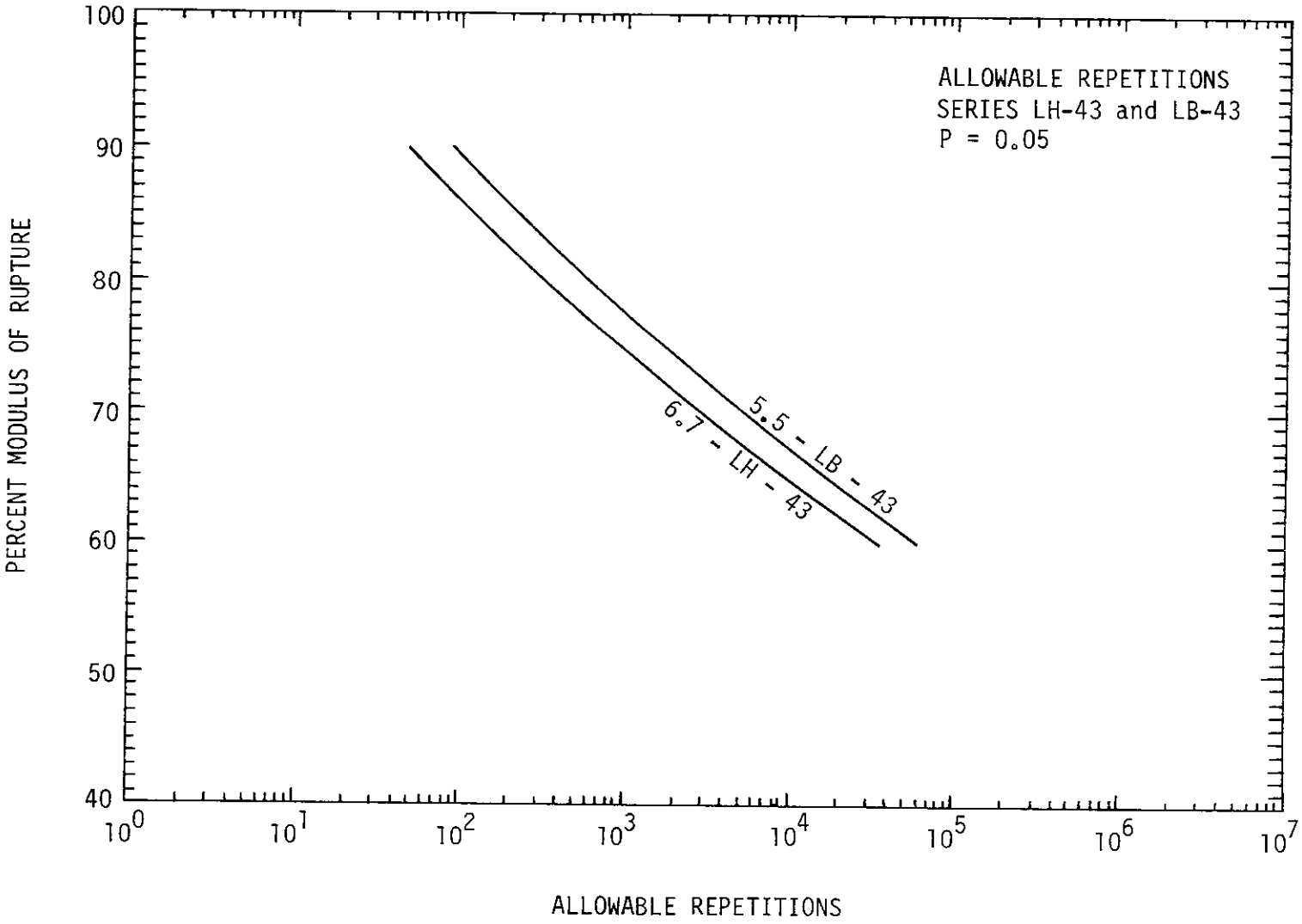

Figure 31. S-N curves showing allowable repetitions for Series LH-43 and LB-43.

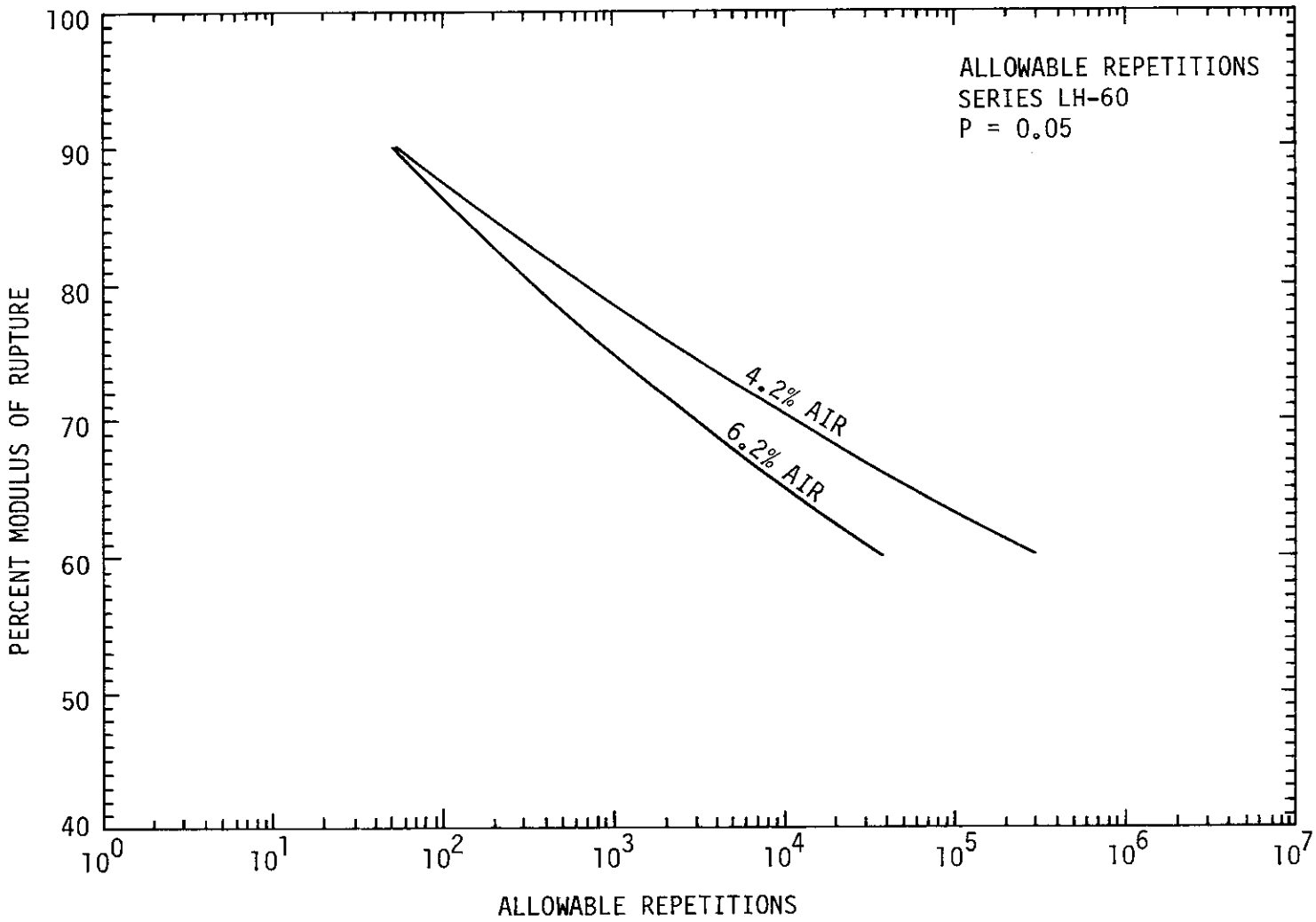

Figure 32. S-N curves showing allowable repetitions for Series LH-60.

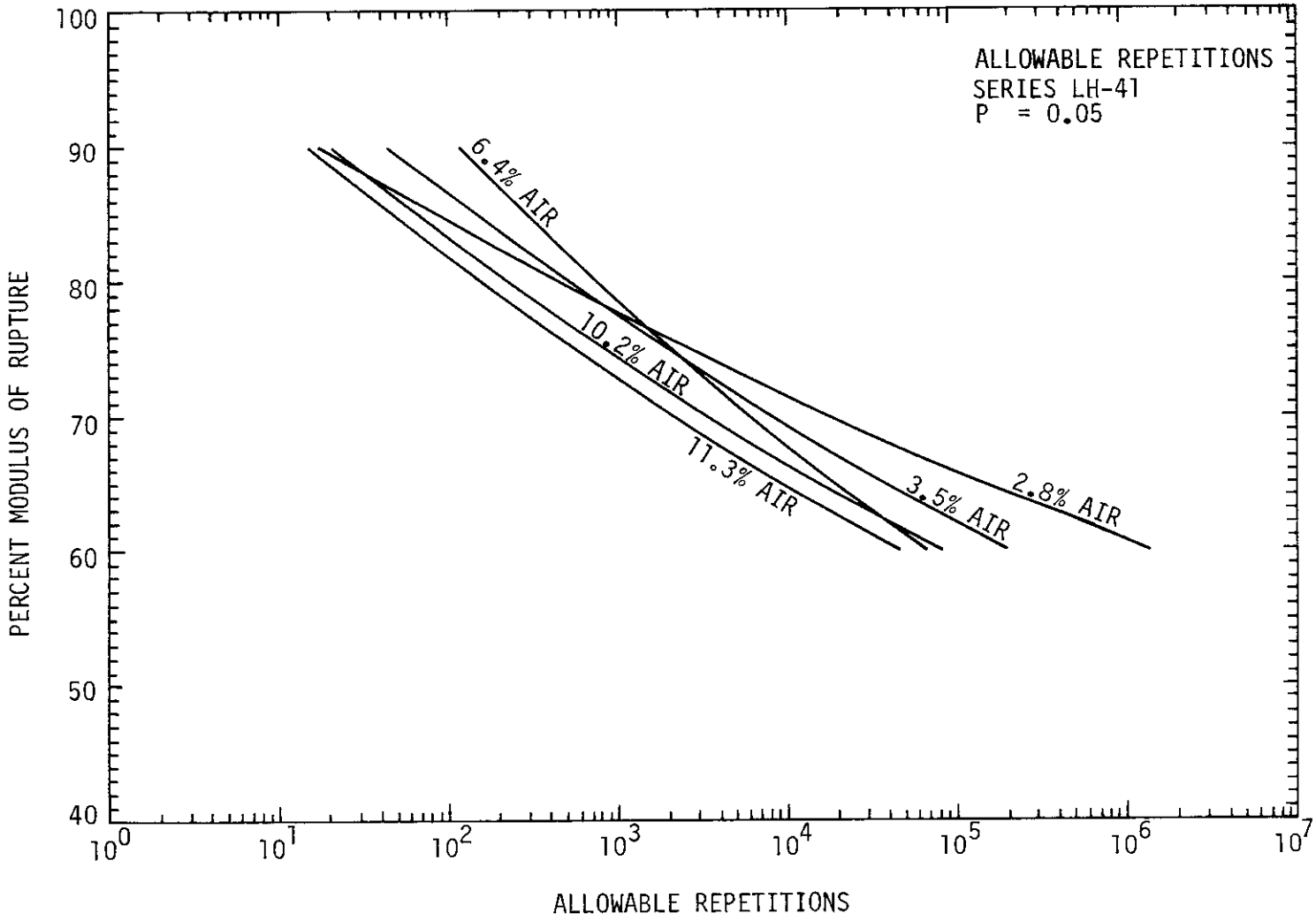

Figure 33. S-N curves showing allowable repetitions for Series LH-41.

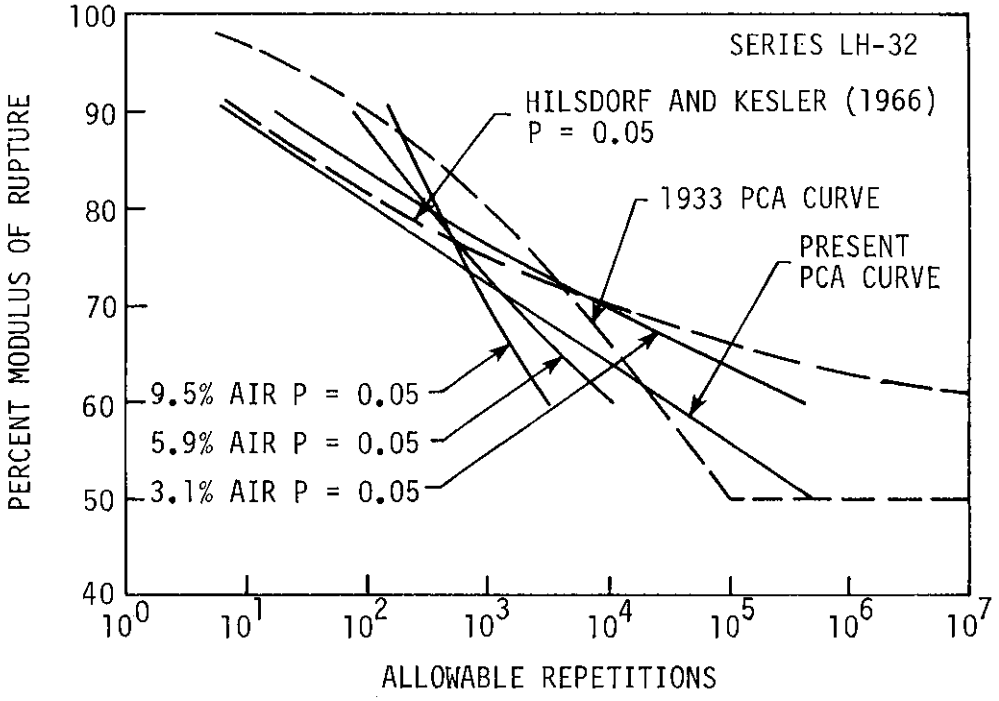

Figure 34. Comparison of pavement fatigue design curves with Series LH-32.

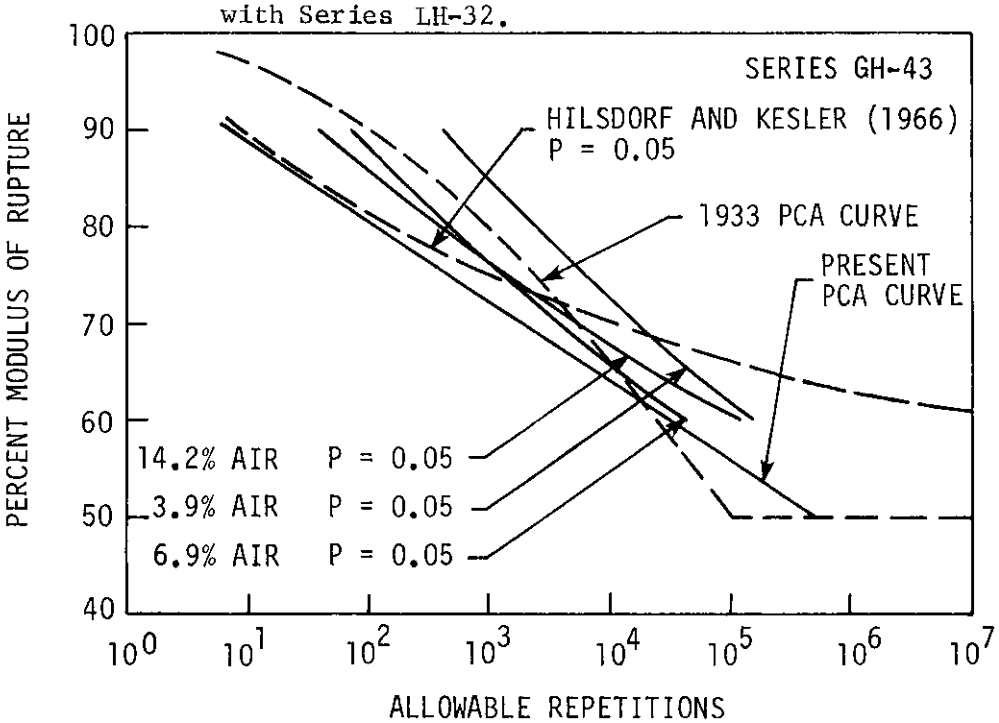

Figure 35. Comparison of pavement fatigue design curves with Series GH-43.

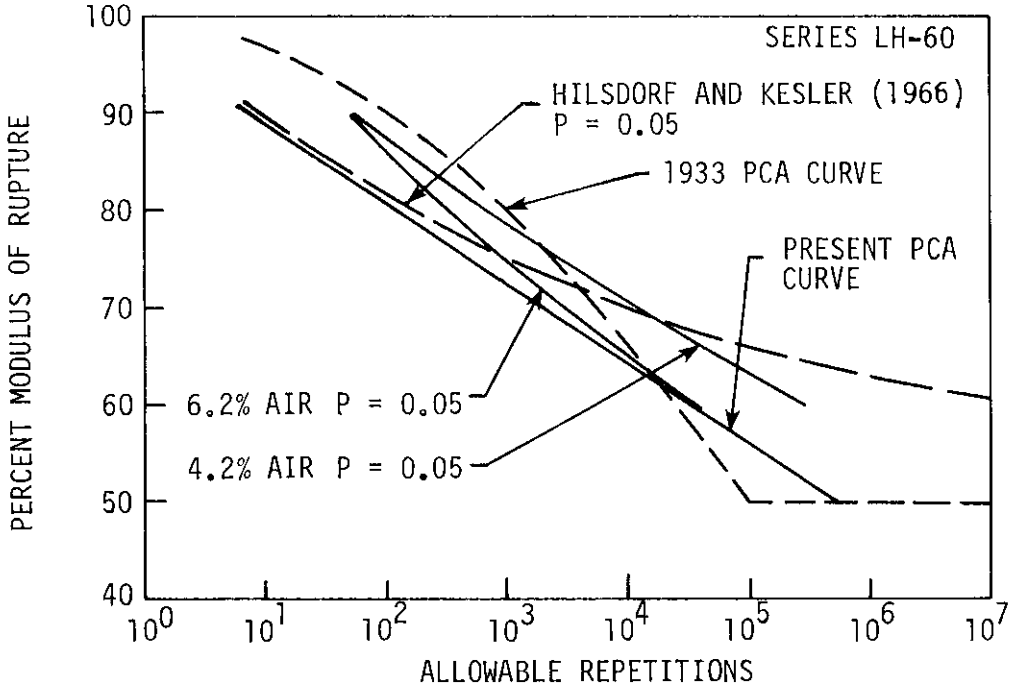

Figure 36. Comparison of pavement fatigue design curves with Series LH-60.

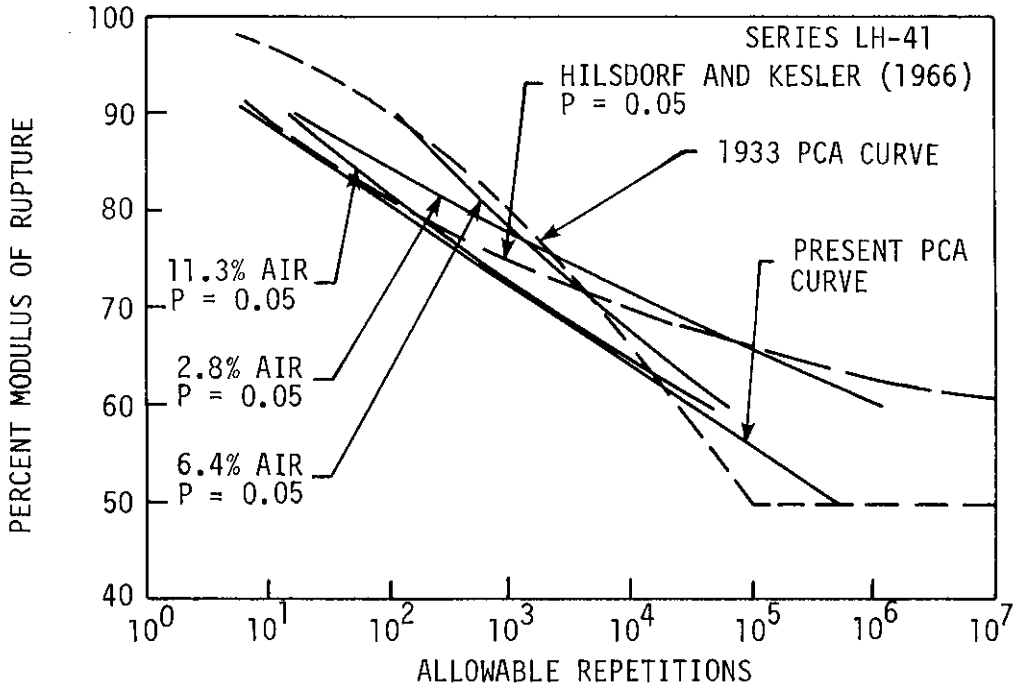

Figure 37. Comparison of pavement fatigue design curves with Series LH-41.

From Figures 34 through 37 it may be observed that the present PCA fatigue curve is conservative with respect to the Hilsdorf and Kesler curve as well as to most of the curves of this study. However, as may be seen in Figure 34, the present PCA curve over estimates the fatigue strength in terms of allowable load applications for a low water-cement ratio, 0.32, at medium to high air contents. In other words, a concrete pavement with a water-cement ratio of 0.32 designed according to the current PCA curve, containing a range of air from 6%-9.5%, could fail prematurely.

To illustrate the effects of air content, water-cement ratio, and aggregate type on thickness requirements, pavement designs were performed using the Iowa DOT Pavement Design Procedure (13) with fatigue curves from this study as well as the standard PCA 1933 and 1966 fatigue curves. The results are compared in terms of the required slab thickness. The same design traffic data and subgrade k values were used in all cases. The fatigue curves that were used are shown in Figures 29-33. The distribution of axle loads during the design life correspond to Design Example Number 2 of reference 33 (see Table D-7 of Appendix D); representative samples of the design calculations are presented in Tables D-8 to D-11 of Appendix D. The effects of air content, water-cement ratio, and aggregate type on the modulus of rupture were taken into account by using modulus of rupture values which could be expected from a given concrete mix based on the results of this study. The results of the thickness design calculations are presented in Table 4.

Table 4. Comparison of pavement thickness design curves

Design No.	Pavement thickness design curve	Assumed modulus of rupture, psi	Pavement thickness required for less than 125% fatigue life consumption, in.	
			Proposed curve	1966 PCA curve
1	1933 PCA	600	10.0	9.5
2	Series 3.1-LH-32	750	7.5	8.0
3	Series 5.9-LH-32	650	9.5	9.0
4	Series 9.5-LH-32	550	11.5	10.5
5	Series 3.9-GH-43	800	7.5	8.0
6	Series 6.9-GH-43	700	8.5	8.5
7	Series 14.2-GH-43	500	10.5	11.0
8	Series 6.7-LH-43	500	11.0	11.0
9	Series 5.5-LB-43	650	9.0	9.0
10	Series 4.2-LH-60	600	9.0	9.5
11	Series 6.2-LH-60	550	10.5	10.5
12	Series 2.8-LH-41	850	6.5	7.5
13	Series 3.5-LH-41	800	7.5	8.0
14	Series 6.4-LH-41	550	10.0	10.5
15	Series 10.2-LH-41	500	10.5	11.0
16	Series 11.3-LH-41	500	11.0	11.0

As may be seen in Table 4, designs utilizing the curves developed in this study, for the selected subgrade and traffic data, give results identical to that obtained by using the 1966 PCA curve in 5 of the 15 cases. In 8 of the 15 cases, the PCA curve requires thicker pavement than designs based on the curves developed in this study, and in two cases, the PCA curve under-designs the pavement thickness by 1/2 to 1 inch.

It should be remembered that these comparisons are based on designs for one set of subgrade and traffic data. The differences could be greater or less for different subgrade and traffic conditions. Reducing the pavement thickness by 1/2-inch may not appear to be a significant savings. However, based on an average pavement width of 24-feet and an average cost of $40 per cubic yard for concrete, a savings of $7800 per mile of concrete paving could be realized by reducing the pavement thickness by 1/2 inch.

Other general observations that can be made from this comparison are:

- For a given water-cement ratio, the pavement thickness required increases with increasing air content.
- For concretes of different water-cement ratios, made with same coarse aggregate at similar air contents, as the water-cement ratio increases, the required pavement thickness increases.
- Concretes made with gravel require the same or less thickness of pavement than the concretes made with limestone at similar air contents and water-cement ratios.

It may be argued that some of the air contents and water-cement ratios used in this comparison are out of the range of normal design for concrete mixes. But this investigation shows that the air content and the water-cement ratio do affect the flexural fatigue strength of plain concrete, and these variables should be considered for optimum design of concrete pavements.

to be applied at the same spacing as the modulus of rupture machine. Two hundred thirty-nine fatigue tests were conducted. Results of these tests are presented in graphic form in the text (Figures 9 through 18) and in tabular form in Appendix B.

The S-N diagrams presented in the text show a reduction in fatigue life as the air content increases and as the water-cement ratio is decreased to 0.32. Curves which are suitable for design are presented in Figures 29 through 33 (tabulated values of these curves are given in Tables D-1 through D-6 in Appendix D). These figures present the allowable repetitions of stress with a constant probability of 0.05. The constant probability of 0.05 means that for 100 specimens tested at a given stress level, only 5 would exhibit a fatigue life less than indicated by the curve.

The fatigue curves developed in this study were used in pavement designs following the Iowa DOT Pavement Design Procedure and compared to designs using the PCA fatigue curves. For the given subgrade and traffic, the thickness required according to the fatigue curves of this study is within one inch of the thickness required according to the Iowa DOT design procedure (which is based on the PCA design curve). The thickness required by the Iowa DOT design procedure is conservative for most cases. However, for a concrete pavement with a water-cement ratio of 0.32 and an air content in the range from 6% to 9.5%, the curves of this study indicated a thickness greater than that required by the current Iowa DOT design procedure.

The main fatigue test program was supplemented by four additional investigations which determined the compressive strength, modulus of rupture, modulus of elasticity, and unit weight for each series.

Conclusions

The following conclusions can be made as a result of the tests performed in this investigation:

1. The fatigue behavior of plain concrete in flexure is affected by the air content of the concrete. The fatigue strength decreases as the air content increases. Fatigue curves obtained from this study (Figures 29-33) provide a basis for improved rigid pavement design.
2. The fatigue behavior of plain concrete in flexure is affected by the water-cement ratio of the concrete. The fatigue strength is decreased for a low water cement ratio (0.32). There did not seem to be a discernible difference in fatigue strength for concretes with a water-cement ratio in the range 0.40 to 0.60.
3. The fatigue behavior of plain concrete in flexure is affected by the coarse aggregate type used in the concrete. At high stress levels, the concrete made with gravel exhibits a higher fatigue strength than that exhibited by the concrete made with limestone. At lower stress levels there does not seem to be a significant difference in fatigue strength.
4. The fatigue behavior of plain concrete in flexure may be affected by the fine aggregate type used in the concrete. There may be a slight increase in fatigue strength when the higher quality fine aggregate is

used. From Figure 21 Series LB-43 seems to exhibit a higher fatigue strength than Series LH-43, although it is difficult to determine whether this trend is significant with the limited data available from this study.

5. As the air content increases the failure of concrete occurs increasingly at the aggregate-cement paste boundary. In other words, as air content rises, failure around the aggregate, as opposed to through the aggregate, predominates.
6. For similar air contents, the failure surface for gravel tends to be at the aggregate-cement paste interface. For limestone, the failure surface seems to pass through the coarse aggregate.
7. The modulus of elasticity, compressive strength, modulus of rupture, and unit weight all generally decrease as the air content of the concrete increases.
8. The modulus of elasticity, compressive strength, modulus of rupture, and unit weight of concrete all decrease as the water-cement ratio increases.
9. For similar air contents, concrete made with gravel has a higher modulus of elasticity, modulus of rupture, and unit weight than concrete made with limestone.

RECOMMENDED FUTURE STUDIES

The present study has shown that air content, water-cement, and aggregate type do affect the flexural fatigue strength of plain concrete. In view of these findings the following areas of flexural fatigue of concrete should be pursued:

- The effects of low and high water-cement ratio on concrete made with gravel.
- The effects of varied water-cement ratio and air contents on concrete made with a high quality sand.
- The effects of air content, water-cement ratio, and aggregate type on reinforced concrete.
- The effects of axial loads on fatigue life.
- The effects of surface treatments (high density surface, polymer, sulfur penetration, etc.) on concrete fatigue life.

LITERATURE CITED

1. AASHTO Interim Guide for Design of Pavement Structures. Washington, D.C.: American Association of State Highway and Transportation Officials, 1974.

2. Al-Rawi, R. S., and K. Al-Murshidi. "Effects of Maximum Size and Surface Texture of Aggregate in Accelerated Testing of Concrete." Cement and Concrete Research, 8 (1978), 201-210.

3. Antrim, J. C., and J. F. McLaughlin. "Fatigue Study of Air Entrained Concrete." American Concrete Institute Journal, Proceedings, 55 (May 1959), 1073-1182.

4. Ballinger, C. A. Effect of Load Variations on the Flexural Fatigue Strength of Plain Concrete. Washington, D.C.: Federal Highway Administration, September, 1972.

5. Bradbury, R. D. Reinforced Concrete Pavements. Washington, D.C.: Wire Reinforcement Institute, 1938.

6. Clemmer, H. F. "Fatigue of Concrete." American Society of Testing and Materials, Proceedings, 22, Part II (1922), 409-419.

7. Concrete and Mineral Aggregates; Manual of Concrete Testing. Philadelphia, Pa.: American Society for Testing and Materials, 1977.

8. Concrete Pavement Design. Chicago, Illinois: Portland Cement Association, 1951.

9. Design and Control of Concrete Mixtures (11th ed.). Skokie, Ill.: Portland Cement Association, 1968.

10. Fordyce, P., and R. G. Packard. "Concrete Pavement Design." Presented to the AASHO Committee on Design, 49th Annual Meeting, October 1963. (Also available from Portland Cement Association, Skokie, Ill.)

11. Fordyce, P., and W. A. Yrjanson. "Modern Techniques for Thickness Design of Concrete Pavements." American Society of Civil Engineers Annual Meeting and National Meeting on Structural Engineering, 1968. (Also available from Portland Cement Association, Skokie, Ill.)

12. Goldbeck, A. T. "The Design of Cement Concrete Pavements." Concrete, 27, No. 3 (September 1925), 22-26.

13. Guide for Primary and Interstate Road Pavement Design. Ames, Ia.: Iowa Department of Transportation, 1976.

14. Hatt, W. K. "Fatigue of Concrete." Highway Research Board, Proceedings, 4 (December 1924), 47-60.

15. Hilsdorf, H. K., and C. E. Kesler. "Fatigue Strength of Concrete Under Varying Flexural Stresses." American Concrete Institute Journal, 63, No. 10 (October 1966), 1059-1075.

16. Kaplan, M. F. "Flexural and Compressive Strength of Concrete as Affected by the Properties of Coarse Aggregates." American Concrete Institute Journal, Proceedings, 55 (May 1959), 1193-1208.

17. Kelley, E. F. "Application of the Results of Research to the Structural Design of Concrete Pavements." Public Roads, 20 (1940), 107-126.

18. Kesler, C. E. "Effect of Speed of Testing on Flexural Fatigue Strength of Plain Concrete." Highway Research Board, Proceedings, 32 (January 1953), 251-258.

19. Kesler, C. E. Significance of Tests and Properties of Concrete-Making Materials. American Society of Testing and Materials: Special Technical Publication 169 A (1966), 144-159.

20. Kosteas, D. "Effect of the Number of Samples on the Statistical and Regression Analysis of Fatigue Tests." Aluminum, 50, No. 2 (1974), 165-170.

21. Lee, D. Y., F. W. Klaiber, and J. W. Coleman. Fatigue Behavior of Air-Entrained Concrete. Ames, Iowa: Engineering Research Institute, Iowa State University, July 1977.

22. McCall, J. T. "Probability of Fatigue Failure of Plain Concrete." American Concrete Institute Journal, Proceedings, 55 (August 1958), 233-244.

23. Mielenz, R. C., V. E. Wolkodoff, J. E. Backstrom, and H. L. Flack. "Origin, Evolution, and Effects of the Air Void System in Concrete. Part I - Entrained Air in Unhardened Concrete." American Concrete Institute, Proceedings, 55 (July 1958), 95-122.

24. Mills, R. E., and R. F. Dawson. "Fatigue of Concrete." Highway Research Board, Proceedings, 7 (December 1927), 160-172.

25. Murdock, J. W., and C. E. Kesler. "Effect of Range of Stress on Fatigue Strength of Plain Concrete Beams." American Concrete Institute Journal, Proceedings, 55 (August 1958), 221-232.

26. Neville, A. M. Properties of Concrete. New York: John Wiley and Sons, Inc., 1973.

27. Nordby, G. M. "Fatigue of Concrete - A Review of Research." American Concrete Institute Journal, Proceedings, 55 (August 1958), 191-220.

28. Older, C. "Bates Experimental Road." State of Illinois, Department of Public Works and Buildings, Divison of Highways, Bulletin No. 18, January 1922.

29. Older, C. "Highway Research in Illinois." American Society of Civil Engineers, Transactions, 87 (1924), 1180-1222.

30. Raithby, K. D., and J. W. Galloway. "Effects of Moisture Condition, Age, and Rate of Loading on Fatigue of Plain Concrete." American Concrete Institute, Publication SP-41 (1974), 15-34.

31. Ray, G. K. "History and Development of Concrete Pavement Design." American Society of Civil Engineers: Journal of the Highway Division, 90 (1964), 79-98.

32. Standard Specifications for Highway and Bridge Construction. Ames, Iowa: Iowa Department of Transportation, 1977.

33. Thickness Design for Concrete Pavements. Skokie, Illinois: Portland Cement Association, 1966.

34. Westergaard, H. M. "Computation of Stresses in Concrete Roads." Highway Research Board, Proceedings, 5, Part I (December 1925), 90-112.

35. Westergaard, H. M. "Stresses in Concrete Pavements Computed by Theoretical Analysis." Public Roads, 7, No. 2 (April 1926), 25-35.

36. Yoder, E. J., and M. W. Witczak. Principals of Pavement Design. New York: John Wiley and Sons, Inc., 1975.

ACKNOWLEDGMENTS

This thesis presents the results of a research program investigating the effects of content, water-cement ratio, and aggregate type on the flexural fatigue strength of plain concrete. The program was conducted by the Engineering Research Institute of Iowa State University and was funded by the Iowa Department of Transportation.

The author wishes to express his appreciation to his co-major professors, Dr. F. W. Klaiber and Dr. Dah Yinn Lee, for their support and guidance throughout the duration of the research effort.

The author wishes to extend sincere appreciation to Dr. Craig Van Nostrand and Neil Werner, Statistics, for their aid in the statistical regression analysis of the fatigue data.

Appreciation is also extended to the engineers of the Iowa DOT for their cooperation and counseling. A special thanks is extended to LaVern Huckstadt for his assistance in running the high pressure air tests.

Special thanks are given to graduate student Cheryl Heyveld and to undergraduate James Julstrom for their assistance in various phases of the project.

APPENDIX A: MATERIAL PROPERTIES AND PROPORTIONS

Table A-1. Gradation of fine aggregate

Sieve size	% passing		
	Bellevue sand	Hallett sand	Iowa D.O.T. specifications
3/8 in.	100	100	100
No. 4	97.0	99.0	90-100
No. 8	74.5	85.2	70-100
No. 16		65.0	
No. 30	42.5	40.2	
No. 50	6.5	8.2	
No. 100	0.5	0.4	
No. 200	0.1	0.1	0-1.5

Table A-2. Gradation of coarse aggregate

Sieve size	% passing		
	Limestone	Gravel	Iowa D.O.T. specifications
1 1/2 in.	100	100	100
1 in.	98.0	91.0	95-100
3/4 in.	70.4	60.2	
1/2 in.	41.0	39.0	25-60
3/8 in.	15.1	19.1	
No. 4	5.0	1.0	0-10
No. 8	2.0	0.5	0-5
No. 200	1.0	0.2	0-1.5

Table A-3. Cement properties

Property	Test value	Specification (ASTM C150 and Fed. SS-C-1960/3)
Chemical data		
SiO_2	22.0	-
AlO_3	5.4	7.5 max.
FeO_3	2.3	-
CaO	64.5	-
MgO	2.3	5.0 max.
SO_3	3.0	3.5 max.
Loss on ignition	1.0	3.0 max.
Insoluable residue	.4	.75 max.
Physical data		
Fineness, Blaine - cm^2/gm	3700	2800 min.
Soundness, Autoclave - %	.04	.80 max.
Time of set, Vicat - minutes		
Initial	80	45 min.
Final	190	480 max.
Air content - %	10	12.0 max./min.
Compressive strength - psi:		
3 day	2900	1800 min.
7 day	3990	2800 min.

Table A-4. Laboratory batch quantities

Series	W/C	Cement, lb	Water,[a] lb	Sand, lb	Coarse aggregate, lb	Ad Aire, ml	Water reducer, ml
23-A	.32	852	318	1507	1731	0	1260
66-A	.32	825	320	1427	1651	186	1220
109-A	.32	971	334	1382	1539	3800	1260
24-1B	.43	640	309	1500	1870	0	0
67-1B	.43	647	307	1479	o841	160	0
1014-1B	.43	578	270	1465	1805	3113	0
67-2B	.43	638	314	1540	1773	200	0
66-3B	.43	638	324	1485	1720	185	0
24-C	.60	440	305	1464	1694	0	0
66-C	.60	451	317	1575	1805	120	0

[a]Includes water required to bring aggregate to saturated surface dry condition.

APPENDIX B: FATIGUE TEST DATA

Table B-1. Fatigue test data for Series 3.1-LH-32

Specimen	Modulus of rupture	Percent modulus of rupture	Fatigue life, number of load applications for failure
3.1-LH-32.1	745	90	639
3.1-LH-32.11	780	90	233
3.1-LH-32.29	795	90	1,040
3.1-LH-32.22	876	90	42
3.1-LH-32.25	780	90	953
3.1-LH-32.16	756	90	434
3.1-LH-32.4	766	80	11,045
3.1-LH-32.26	762	80	80,091
3.1-LH-32.12	835	80	401
3.1-LH-32.1	738	80	9,440
3.1-LH-32.23	823	80	3,740
3.1-LH-32.15	833	80	4,300
3.1-LH-32.2	728	70	1,208,300[a]
3.1-LH-32.10	784	70	34,520
3.1-LH-32.27	779	70	95,190
3.1-LH-32.21	790	70	830,880
3.1-LH-32.6	746	70	47,970
3.1-LH-32.14	788	70	48,440
3.1-LH-32.19	769	65	2,106,900[a]
3.1-LH-32.7	740	65	114,440
3.1-LH-32.24	798	65	2,102,920[a]
3.1-LH-32.17	838	65	11,920
2.1-LH-32.3	736	60	2,050,000[a]
3.1-LH-32.28	799	60	2,098,690[a]
3.1-LH-32.8	735	60	2,138,440[a]
3.1-LH-32.13	848	60	2,187,540[a]

[a]Specimen did not fail.

Table B-2. Fatigue test data for Series 5.9-LH-32

Specimen	Modulus of rupture, psi	Percent modulus of rupture	Fatigue life, number of load applications for failure
5.9-LH-32.14	665	90	170
5.9-LH-32.7	620	90	640
5.9-LH-32.28	640	90	950
5.9-LH-32.10	690	90	540
5.9-LH-32.6	650	90	290
5.9-LH-32.20	680	90	610
5.9-LH-32.17	650	80	1,960
5.9-LH-32.12	610	80	1,640
5.9-LH-32.29	660	80	850
5.9-LH-32.4	620	80	2,060
5.9-LH-32.22	680	80	1,770
5.9-LH-32.26	715	80	2,150
5.9-LH-32.13	660	70	8,400
5.9-LH-32.8	640	70	2,890
5.9-LH-32.30	700	70	8,790
5.9-LH-32.11	700	70	6,800
5.9-LH-32.5	590	70	13,430
5.9-LH-32.23	690	70	15,690
5.9-LH-32.16	645	60	24,280
5.9-LH-32.14	655	60	19,500
5.9-LH-32.27	690	60	18,670
5.9-LH-32.24	680	60	79,880
5.9-LH-32.9	610	60	3,032,130[a]
5.9-LH-32.3	640	60	32,280

[a]Specimen did not fail.

Table B-3. Fatigue test data for Series 9.5-LH-32

Specimen	Modulus of rupture, psi	Percent modulus of rupture	Fatigue life, number of load applications for failure
9.5-LH-32.21	542	90	540
9.5-LH-32.29	585	90	430
9.5-LH-32.6	470	90	1,530
9.5-LH-32.16	514	90	510
9.5-LH-32.7	542	90	230
9.5-LH-32.11	640	90	180
9.5-LH-32.24	529	80	1,250
9.5-LH-32.26	569	80	790
9.5-LH-32.2	578	80	660
9.5-LH-32.15	545	80	620
9.5-LH-32.18	540	80	950
9.5-LH-32.20	578	80	1,320
9.5-LH-32.23	539	70	3,440
9.5-LH-32.28	575	70	5,960
9.5-LH-32.19	555	70	4,330
9.5-LH-32.5	540	70	3,040
9.5-LH-32.25	585	70	3,990
9.5-LH-32.10	585	70	3,260
9.5-LH-32.22	554	60	15,450
9.5-LH-32.27	554	60	12,100
9.5-LH-32.4	553	60	10,170
9.5-LH-32.9	544	60	7,410
9.5-LH-32.13	600	60	8,510
9.5-LH-32.12	575	60	8,370

Table B-4. Fatigue test data for Series 3.9-GH-43

Specimen	Modulus of rupture, psi	Percent modulus of rupture	Fatigue life, number of load applications for failure
3.9-GH-43.25	845	90	4,210
3.9-GH-43.10	825	90	3,570
3.9-GH-43.15	825	90	1,870
3.9-GH-43.6	860	90	1,340
3.9-GH-43.24	860	90	3,240
3.9-GH-43.23	800	80	22,660
3.9-GH-43.16	885	80	12,710
3.9-GH-43.18	860	80	8,400
3.9-GH-43.5	790	80	7,240
3.9-GH-43.12	840	80	12,130
3.9-GH-43.14	860	70	51,180
3.9-GH-43.27	835	70	33,190
3.9-GH-43.22	853	70	65,170
3.9-GH-43.11	800	70	62,050
3.9-GH-43.8	810	70	127,490
3.9-GH-43.20	840	60	1,287,300
3.9-GH-43.26	890	60	257,570
3.9-GH-43.13	850	60	2,316,280[a]
3.9-GH-43.4	800	60	2,138,260[a]
3.9-GH-43.29	940	60	2,112,750[a]

[a]Specimen did not fail.

Table B-5. Fatigue test data for Series 6.9-GH-43

Specimen	Modulus of rupture, psi	Percent modulus of rupture	Fatigue life, number of load applications for failure
6.9-GH-43.23	755	90	200
6.9-GH-43.25	715	90	940
6.9-GH-43.18	775	90	1,620
6.9-GH-43.29	760	90	280
6.9-GH-43.13	700	90	1,760
6.9-GH-43.4	759	90	300
6.9-GH-43.20	700	80	1,980
6.9-GH-43.22	730	80	2,490
6.9-GH-43.16	765	80	880
6.9-GH-43.28	702	80	5,190
6.9-GH-43.9	745	80	1,340
6.9-GH-43.3	720	80	1,250
6.9-GH-43.21	730	70	59,090
6.9-GH-43.17	728	70	23,100
6.9-GH-43.30	745	70	17,290
6.9-GH-43.26	728	70	55,000
6.9-GH-43.2	690	70	30,640
6.9-GH-43.7	745	70	4,880
6.9-GH-43.19	710	60	1,614,640[a]
6.9-GH-43.27	748	60	30,060
6.9-GH-43.1	700	60	144,830
6.9-GH-43.11	787	60	137,180
6.9-GH-43.15	710	60	1,123,220[a]

[a]Specimen did not fail.

Table B-6. Fatigue test data for Series 14.2-GH-43

Specimen	Modulus of rupture, psi	Percent modulus of rupture	Fatigue life, number of load applications for failure
14.2-GH-43.21	415	90	910
14.2-GH-43.18	430	90	740
14.2-GH-43.14	436	90	350
14.2-GH-43.9	395	90	520
14.2-GH-43.28	400	90	2,170
14.2-GH-43.25	372	90	2,370
14.2-GH-43.23	440	80	1,950
14.2-GH-43.19	440	80	4,020
14.2-GH-43.13	440	80	22,030
14.2-GH-43.2	436	80	5,200
14.2-GH-43.16	446	80	16,370
14.2-GH-43.10	445	80	400
14.2-GH-43.24	430	70	6,670
14.2-GH-43.17	451	70	25,310
14.2-GH-43.29	400	70	19,280
14.2-GH-43.12	450	70	77,160
14.2-GH-43.7	460	70	16,920
14.2-GH-43.6	455	70	2,580
14.2-GH-43.1	450	65	946,530
14.2-GH-43.26	411	65	46,970
14.2-GH-43.20	450	60	2,507,790[a]
14.2-GH-43.30	427	60	3,065,610[a]
14.2-GH-43.15	445	60	2,039,420[a]
14.2-GH-43.11	426	60	2,702,980[a]

[a]Specimen did not fail.

Table B-7. Fatigue test data for Series 6.7-LH-43

Specimen	Modulus of rupture, psi	Percent modulus of rupture	Fatigue life, number of load applications for failure
6.7-LH-43.1	520	90	440
6.7-LH-43.21	544	90	210
6.7-LH-43.27	505	90	680
6.7-LH-43.17	535	90	270
6.7-LH-43.23	490	90	1,350
6.7-LH-43.8	520	90	810
6.7-LH-43.2	529	80	2,830
6.7-LH-43.20	495	80	3,250
6.7-LH-43.28	534	80	1,810
6.7-LH-43.16	525	80	5,230
6.7-LH-43.9	543	80	4,000
6.7-LH-43.13	530	80	2,120
6.7-LH-43.24	515	70	7,640
6.7-LH-43.18	550	70	7,170
6.7-LH-43.22	529	70	5,700
6.7-LH-43.10	537	70	32,770
6.7-LH-43.14	490	70	24,830
6.7-LH-43.3	565	70	8,450
6.7-LH-43.11	505	60	2,122,260[a]
6.7-LH-43.25	530	60	105,160
6.7-LH-43.15	530	60	70,970
6.7-LH-43.4	518	60	2,031,950[a]
6.7-LH-43.7	570	60	23,810
6.7-LH-43.19	530	60	2,996,910[a]

[a]Specimen did not fail.

Table B-8. Fatigue test data for Series 5.5-LB-43

Specimen	Modulus of rupture, psi	Percent modulus of rupture	Fatigue life, number of load applications for failure
5.5-LB-43.25	608	90	2,260
5.5-LB-43.29	680	90	480
5.5-LB-43.21	642	90	580
5.5-LB-43.18	657	90	2,620
5.5-LB-43.1	645	90	630
5.5-LB-43.9	707	90	300
5.5-LB-43.19	666	80	4,820
5.5-LB-43.26	654	80	1,190
5.5-LB-43.13	608	80	2,470
5.5-LB-43.10	671	80	1,640
5.5-LB-43.6	657	80	2,210
5.5-LB-43.16	688	80	5,900
5.5-LB-43.20	653	70	18,290
5.5-LB-43.30	633	70	40,820
5.5-LB-43.27	662	70	43,330
5.5-LB-43.8	655	70	28,400
5.5-LB-43.17	678	70	11,770
5.5-LB-43.2	668	70	76,500
5.5-LB-43.28	652	60	2,195,190[a]
5.5-LB-43.22	720	60	157,800
5.5-LB-43.14	673	60	107,530
5.5-LB-43.9	660	60	2,199,280[a]
5.5-LB-43.3	668	60	2,148,830[a]
5.5-LB-43.11	679	60	51,920
5.5-LB-43.5	710	60	107,930

[a]Specimen did not fail.

Table B-9. Fatigue test data for Series 4.2-LH-60

Specimen	Modulus of rupture, psi	Percent modulus of rupture	Fatigue life, number of load applications for failure
4.2-LH-60.17	580	90	1,060
4.2-LH-60.21	635	90	210
4.2-LH-60.24	617	90	740
4.2-LH-60.27	595	90	1,010
4.2-LH-60.2	610	90	420
4.2-LH-60.9	675	90	420
4.2-LH-60.18	610	80	960
4.2-LH-60.22	600	80	1,960
4.2-LH-60.25	660	80	1,080
4.2-LH-60.29	635	80	1,940
4.2-LH-60.3	625	80	1,150
4.2-LH-60.8	630	80	4,320
4.2-LH-60.19	632	70	21,740
4.2-LH-60.23	578	70	366,830
4.2-LH-60.26	590	70	1,075,160
4.2-LH-60.1	683	70	26,380
4.2-LH-60.10	653	70	53,190
4.2-LH-60.15	625	70	117,120
4.2-LH-60.16	595	60	1,233,530[a]
4.2-LH-60.20	660	60	385,160
4.2-LH-60.28	614	60	2,034,460[a]
4.2-LH-60.4	652	60	935,460
4.2-LH-60.7	645	60	2,035,170[a]
4.2-LH-60.11	620	60	1,595,560

[a]Specimen did not fail.

Table B-10. Fatigue test data for Series 6.2-LH-60

Specimen	Modulus of rupture, psi	Percent modulus of rupture	Fatigue life, number of load applications for failure
6.2-LH-60.23	605	90	212
6.2-LH-60.16	545	90	426
6.2-LH-60.26	590	90	128
6.2-LH-60.5	588	90	456
6.2-LH-60.7	547	90	1,975
6.2-LH-60.19	573	90	502
6.2-LH-60.20	547	80	13,300
6.2-LH-60.17	573	80	1,510
6.2-LH-60.25	579	80	1,261
6.2-LH-60.2	538	80	1,310
6.2-LH-60.14	520	80	3,930
6.2-LH-60.6	555	80	5,054
6.2-LH-60.22	550	70	12,430
6.2-LH-60.18	553	70	16,360
6.2-LH-60.24	580	70	18,250
6.2-LH-60.28	580	70	12,260
6.2-LH-60.1	580	70	2,930
6.2-LH-60.8	574	70	14,340
6.2-LH-60.21	585	60	2,013,440[a]
6.2-LH-60.27	560	60	2,103,800[a]
6.2-LH-60.15	540	60	1,565,880
6.2-LH-60.3	608	60	98,860
6.2-LH-60.12	580	60	100,080
6.2-LH-60.10	544	60	60,130
6.2-LH-60.13	591	60	78,330

[a]Specimen did not fail.

APPENDIX C: STATISTICAL REGRESSION ANALYSIS

There is an area of statistics which deals with fitting a regression equation to a set of observations in which the experiment was stopped, or "censored," before all of the observations were made; it is only known that the observations occur at a later time. Situations where the test is stopped before the observation is made occur in medical research where some small percentage of the test animals live beyond the end of the test, or another example is in fatigue research where the specimens at a low stress level do not fail.

When observations are made at one level and some of them are censored, a weighted average can be made and a value can be assigned to the set of data considering all observations. The theory has been available for sometime, but implementing it into a computer program is a recent development. The program CENSOR which was utilized in this investigation was developed by Dr. William Meeker, Associate Professor of Statistics at Iowa State University.

The equations of the curves shown in Figures 9 through 28 in the text of this report are of the form:

$$\text{Log}(N) = b_0 + b_1 \text{ Log}(S)$$

where

N = number of cycles to failure

b_0 = y-intercept of the curve

b_1 = slope of the curve

S = percent modulus of rupture (i.e., 90, 80, ...)

The slopes and y-intercepts of the curves are given in Table C1. Series 9.5-LH-32 was the only series in which all of the specimens failed,

It should be noted that the above procedure has some error involved. When working with a log scale, a small error in the log value could result in a large error in the arithmetic value. The above procedure should thus be used with caution, and if the cycles to failure are desired for an air content corresponding to an air content in this study, the equations for those curves should be used.

APPENDIX D: PAVEMENT DESIGN

Table D-1. Percent modulus of rupture and allowable load repetitions for Series LH-32

Percent modulus of rupture	Allowable repetitions, percent air		
	3.1	5.9	9.5
60	434410	11074	3180
61	287740	9049	2828
62	191161	7405	2520
63	128469	6093	2248
64	86338	5014	2008
65	58668	4148	1796
66	40133	3443	1609
67	27441	2858	1442
68	18980	2385	1295
69	13204	1996	1164
70	9185	1671	1047
71	6427	1402	944
72	4549	1184	851
73	3220	999	768
74	2292	846	694
75	1636	717	628
76	1175	609	569
77	846	519	516
78	613	443	468
79	446	379	425
80	325	325	386
81	238	279	351
82	176	240	320
83	129	206	292
84	96	178	266
85	71	154	243
86	53	134	222
87	40	116	203

Table D-1. (Continued)

Percent modulus of rupture	Allowable repetitions, percent air		
	3.1	5.9	9.5
88	30	101	186
89	23	88	170
90	17	77	156

Table D-2. Percent modulus of rupture and allowable load repetitions for Series GH-43

Percent modulus of rupture	Allowable repetitions, percent air		
	3.1	5.9	9.5
60	160509	45061	119784
61	126386	34714	86437
62	99701	26798	62517
63	79177	20835	45635
64	62878	16199	33312
65	50246	12682	24524
66	40318	9972	18155
67	32344	7840	13434
68	26116	6207	10032
69	21159	4934	7527
70	17144	3921	5647
71	13938	3128	4255
72	11405	2512	3236
73	9335	2019	2461
74	7663	1628	1880
75	6301	1315	1439
76	5202	1066	1108
77	4300	866	854
78	3566	706	661

Table D-3. Percent modulus of rupture and allowable load repetitions for Series 6.7-LH-43

Percent modulus of rupture	Allowable repetitions, percent air 6.7	Percent modulus of rupture	Allowable repetitions, percent air 6.7
60	35818	76	754
61	27365	77	608
62	20956	78	493
63	16162	79	401
64	12468	80	326
65	9687	81	266
66	7560	82	218
67	5898	83	178
68	4637	84	147
69	3658	85	121
70	2886	86	100
71	2286	87	83
72	1824	88	69
73	1455	89	57
74	1166	90	48
75	935		

Table D-4. Percent modulus of rupture and allowable load repetitions for Series 5.5-LB-43

Percent modulus of rupture	Allowable repetitions, percent air 6.7	Percent modulus of rupture	Allowable repetitions, percent air 6.7
60	59498	76	1335
61	45667	77	1081
62	35124	78	879
63	27208	79	717
64	21081	80	585
65	16448	81	479
66	12888	82	394
67	10097	83	324
68	7969	84	267
69	6311	85	221
70	4999	86	183
71	3975	87	152
72	3183	88	126
73	2550	89	106
74	2050	90	88
75	1650		

Table D-5. Percent modulus of rupture and allowable load repetitions for Series LH-60

Percent modulus of rupture	Allowable repetitions, percent air		Percent modulus of rupture	Allowable repetitions, percent air	
	4.2	6.2		4.2	6.2
60	301856	36906	76	1980	791
61	212716	28242	77	1498	639
62	150245	21647	78	1138	518
63	107152	16722	79	870	422
64	76436	12915	80	665	344
65	55030	10046	81	510	281
66	39847	7851	82	393	230
67	28840	6132	83	303	189
68	21081	4826	84	235	155
69	15485	3812	85	183	128
70	11374	3011	86	143	105
71	8397	2387	87	112	88
72	6259	1907	88	87	73
73	4666	1524	89	69	61
74	2622	981	90	54	51
75	2622	981			

Table D-7. Pavement design axle loads

Axle load groups, kips	Axle loads in design life (33)
Single	
28-30	3,700
26-28	3,700
24-26	7,410
22-24	195,000
20-22	764,400
18-20	2,139,150
16-18	2,870,400
Tandem	
52-54	3,700
50-52	3,700
48-50	36,270
46-48	36,270
44-46	57,530
42-44	179,790
40-42	204,750
38-40	296,400
36-38	319,800
34-36	487,500
32-34	610,350
30-32	1,078,350
Total trucks	19,500,000

Table D-8. Design example - Series LH-32.

CALCULATION OF CONCRETE PAVEMENT THICKNESS
(Use with Case I Single & Tandem Axle Design Charts)

Project Design Example - Series LH-32

Type _____ No. of Lanes _____

Subgrade k 100 pci., Subbase _____

Combined k 130 pci., Load Safety Factor 1.2 (L.S.F.)

PROCEDURE

1. Fill in Col. 1,2 and 6, listing axle loads in decreasing order.
2. Assume 1st trial depth. Use 1/2-in. increments.
3. Analyze 1st trial depth by completing columns 3,4,5 and 7.
4. Analyze other trial depths, varying M.R.*, slab depth and subbase type.**

1	2	3	4	5	6	7
Axle Loads kips	Axle Loads X L.S.F. kips	Stress psi	Stress Ratios	Allowable Repetitions No.	Expected Repetitions No.	Fatigue Resistance Used*** percent

Trial depth 7.0 in. M.R.* 750 psi k 130 pci

SINGLE AXLES

30	36.0	480	0.64	86,000	3,700	4.3
28	33.6	460	0.61	290,000	3,700	1.3
26	31.2	435	0.58	1,000,000[a]	7,410	0.7
24	28.8	410	0.55	3,800,000[a]	195,000	5.1
22	26.4	380	0.51	28,000,000[a]	764,400	2.7
20	24.0	350	0.47	Unlimited		

TANDEM AXLES

54	64.8	530	0.71	6,400	3,700	57.8
52	62.4	515	0.69	13,000	3,700	28.5
50	60.0	500	0.67	27,000	36,270	134.3
48	57.6	480	0.64	86,000	36,270	42.2
46	55.2	465	0.62	190,000	57,530	30.3
44	52.8	450	0.60	430,000	179,790	41.8
42	50.4	430	0.57	1,600,000[a]	204,750	12.8
40	48.0	410	0.55	3,800,000[a]	296,400	7.8
38	45.6	395	0.53	11,000,000[a]	319,800	2.9
36	43.2	375	0.50	Unlimited		

Total = 372.5%

* M.R. Modulus of Rupture for 3rd pt. loading.

** Cement-treated subbases result in greatly increased combined k values.

*** Total fatigue resistance used should not exceed about 125 percent.

[a] Extrapolated value.

Table D-9. Design example - Series LH-32.

CALCULATION OF CONCRETE PAVEMENT THICKNESS
(Use with Case I Single & Tandem Axle Design Charts)

Project Design Example - Series LH-32 No. of Lanes _____

Type _____

Subgrade k 100 pci., Subbase _____

Combined k 130 pci., Load Safety Factor 1.2 (L.S.F.)

PROCEDURE

1. Fill in Col. 1,2 and 6, listing axle loads in decreasing order.
2. Assume 1st trial depth. Use 1/2-in. increments.
3. Analyze 1st trial depth by completing columns 3,4,5 and 7.
4. Analyze other trial depths, varying M.R.*, slab depth and subbase type.**

1	2	3	4	5	6	7
Axle Loads kips	Axle Loads X L.S.F. kips	Stress psi	Stress Ratios	Allowable Repetitions No.	Expected Repetitions No.	Fatigue Resistance Used*** percent
Trial depth 7.5 in. M.R.* 750 psi k 130 pci						
SINGLE AXLES						
30	36.0	440	0.59	640,000[a]	3,700	0.6
28	33.6	420	0.56	2,400,000[a]	3,700	0.2
26	31.2	395	0.53	11,000,000[a]	7,410	0.1
24	28.8	370	0.49	Unlimited		
TANDEM AXLES						
54	64.8	485	0.65	59,000	3,700	6.3
52	62.4	475	0.63	130,000	3,700	2.8
50	60.0	460	0.61	290,000	36,270	12.5
48	57.6	440	0.59	640,000[a]	36,270	5.7
46	55.2	430	0.57	1,600,000[a]	57,530	3.6
44	52.8	410	0.55	3,800,000[a]	179,790	4.7
42	50.4	395	0.53	11,000,000[a]	204,750	1.9
40	48.0	375	0.50	Unlimited		

Total 38.4%

* M.R. Modulus of Rupture for 3rd pt. loading.

** Cement-treated subbases result in greatly increased combined k values.

*** Total fatigue resistance used should not exceed about 125 percent.

[a] Extrapolated value.

Table D-10. Design example - 1966 PCA design curve.

CALCULATION OF CONCRETE PAVEMENT THICKNESS
(Use with Case I Single & Tandem Axle Design Charts)

Project Design Example - PCA Design Curve No. of Lanes ____

Type ____

Subgrade k 100 pci., Subbase ____

Combined k 130 pci., Load Safety Factor 1.2 (L.S.F.)

PROCEDURE

1. Fill in Col. 1, 2 and 6, listing axle loads in decreasing order.
2. Assume 1st trial depth. Use 1/2-in. increments.
3. Analyze 1st trial depth by completing columns 3, 4, 5 and 7.
4. Analyze other trial depths, varying M.R.*, slab depth and subbase type.**

1	2	3	4	5	6	7
Axle Loads kips	Axle Loads X L.S.F. kips	Stress psi	Stress Ratios	Allowable Repetitions No.	Expected Repetitions No.	Fatigue Resistance Used*** percent

Trial depth 7.5 in. M.R.* 750 psi k 130 pci

SINGLE AXLES

30	36.0	440	0.59	42,000	3,700	8.8
28	33.6	420	0.56	100,000	3,700	3.7
26	31.2	395	0.53	240,000	7,410	3.1
24	28.8	370	0.49	Unlimited		

TANDEM AXLES

54	64.8	485	0.65	8,000	3,700	46.3
52	62.4	475	0.63	14,000	3,700	26.4
50	60.0	460	0.61	24,000	36,270	151.1
48	57.6	440	0.59	42,000	36,270	86.4
46	55.2	430	0.57	75,000	57,530	76.7
44	52.8	410	0.55	130,000	179,790	138.3
42	50.4	395	0.53	240,000	204,750	85.3
40	48.0	375	0.50	Unlimited		

Total = 626.1%

* M.R. Modulus of Rupture for 3rd pt. loading.

** Cement-treated subbases result in greatly increased combined k values.

*** Total fatigue resistance used should not exceed about 125 percent.

Table D-11. Design example - 1966 PCA design curve.

CALCULATION OF CONCRETE PAVEMENT THICKNESS
(Use with Case I Single & Tandem Axle Design Charts)

Project Design Example - PCA Design Curve

Type _____ No. of Lanes _____

Subgrade k 100 pci., Subbase _____

Combined k 130 pci., Load Safety Factor 1.2 (L.S.F.)

PROCEDURE

1. Fill in Col. 1, 2 and 6, listing axle loads in decreasing order.
2. Assume 1st trial depth. Use 1/2-in. increments.
3. Analyze 1st trial depth by completing columns 3, 4, 5 and 7.
4. Analyze other trial depths, varying M.R.*, slab depth and subbase type.**

1	2	3	4	5	6	7
Axle Loads kips	Axle Loads X L.S.F. kips	Stress psi	Stress Ratios	Allowable Repetitions No.	Expected Repetitions No.	Fatigue Resistance Used *** percent

Trial depth 8.0 in. M.R.* 750 psi k 130 pci

SINGLE AXLES

30	36.0	400	0.53	240,000	3,700	1.5
28	33.6	385	0.51	400,000	3,700	0.9
26	31.2	365	0.49	Unlimited		

TANDEM AXLES

54	64.8	445	0.59	42,000	3,700	8.8
52	62.4	435	0.58	57,000	3,700	6.5
50	60.0	420	0.56	100,000	36,270	36.3
48	57.6	405	0.54	180,000	36,270	20.2
46	55.2	390	0.52	300,000	57,530	19.2
44	52.8	375	0.50	Unlimited		

Total = 93.4%

* M.R. Modulus of Rupture for 3rd pt. loading.

** Cement-treated subbases result in greatly increased combined k values.

*** Total fatigue resistance used should not exceed about 125 percent.